Numerical Investigation of Friction and Wear Characteristics of Surfaces using MoS_2 Nanoparticles in PAO

Author

Hafiz Zia ur Rahman

00000274875

Supervisor

Dr. Raja Amer Azim

DEPARTMENT OF MECHANICAL ENGINEERING COLLEGE OF ELECTRICAL & MECHANICAL ENGINEERING NATIONAL UNIVERSITY OF SCIENCES AND TECHNOLOGY ISLAMABAD

AUGUST, 2021

Numerical Investigation of Friction and Wear Characteristics of Surfaces using MoS_2 Nanoparticles in PAO

Author

Hafiz Zia ur Rahman

00000274875

A thesis submitted in partial fulfillment of the requirements for the degree of

MS Mechanical Engineering

Thesis Supervisor

Dr. Raja Amer Azim

DEPARTMENT OF MECHANICAL ENGINEERING

COLLEGE OF ELECTRICAL & MECHANICAL ENGINEERING

NATIONAL UNIVERSITY OF SCIENCES AND TECHNOLOGY

ISLAMABAD

AUGUST, 2021

Declaration

I certify that this research work titled *"Numerical Investigation of Friction and Wear Characteristics of Surfaces using MoS_2 Nanoparticles in PAO*" is my own work. The work has not been presented elsewhere for assessment. The material that has been used from other sources has been properly acknowledged and cited.

Hafiz Zia ur Rahman

00000274875

MS-2018 Mechanical Engineering

College of Electrical & Mechanical Engineering

National University of Sciences and Technology, Islamabad

Language Correctness Certificate

This thesis has been read by an English expert and is free of typing, syntax, semantic, grammatical, and spelling mistakes. The thesis is also written according to the format provided by the university.

Hafiz Zia ur Rahman

00000274875

MS-2018 Mechanical Engineering

College of Electrical & Mechanical Engineering

National University of Sciences and Technology, Islamabad

Dr. Raja Amer Azim

Assistant Professor

Department of Mechanical Engineering

College of Electrical & Mechanical Engineering

National University of Sciences and Technology, Islamabad

Copyright Statement

Acknowledgements

I am immensely grateful to my thesis supervisor, Dr. Raja Amer Azim, for his support, continuous encouragement and constructive criticism that has enabled me to successfully complete my thesis. I am also thankful to him for his guidance and advice regarding research and career prospects during and after my MS studies.

I would also like to express my heartfelt gratitude to Dr. Rehan Zahid for providing invaluable guidance and feedback during this work, and for being on my thesis guidance and evaluation committee. Thanks also go out to Dr.Tariq Talha and Dr. Hasan Aftab Saeed for being a part of this committee.

I would like to extend my gratitude to my colleague, Mr. Faraz Kaiser Malik, for several enlightening discussions. The support of the staff at the Supercomputing Research and Education Center in the Research Center for Modeling and Simulation, National University of Sciences and Technology, is also gratefully acknowledged, as is the kind permission for the use of the facilities at this center.

Dedicated to my beloved parents for their invaluable support and cooperation.

Abstract

Reduction of friction and wear is an ongoing challenge in design and operation of machines and implanted joints. Wear shorten the life of contacting parts. Inclusion of nanoparticles in modern era has emerged as promising solution. Various nanoparticles act as lubricant additives like silver, diamond and copper oxide nanoparticles. Many lubricants are used as base lubricants like dodecane, mineral base oil, polyethylene glycol, fully formulated oil and polyalfaolefin oil. Molybdenum disulfide MoS_2 particles are modeled in Polyalphaolefin base oil. The effect of MoS_2 nanoparticles on real contact area has also been modeled. There is suitable concentration below which nanoparticles cannot reduced friction force. On the basis of results it is stated that nanoparticles have dual effect. Inclusion of direct and indirect method to solve overall contact problem.

To study the effect of addition of nanoparticles in synthetic base oils, a mathematical model has been formulated. It is a multisacle model comprising a rough surface sub contact model and statistical sub contact model. Rough surface contact model are based on micrometer sized roughness features while statistical contact model are based on modeling of nanoparticles in between rough surfaces. This contact model can also be used for other nanoparticles of same size and roughness.

The model is verified using existing experimental data. Parametric study is done, varying the load, particle size and particle weight fraction. COF and wear is evaluated and discussed.

Key Words: *Nanolubricant, Nanoparticle, real area of contact, lubricants, PAO*

Table of Contents

List of Figures

List of Symbols

A_{NP} = contact area for single nanoparticle

A_p = contact area of particles

A_S = contact area between surfaces

A_V = void area instigated by the surfaces

A_{CS} = interference cross-sectional area of particle/surface

A_{void} = void area of single nanoparticle

A_n = apparent area of contact

a = contact radius of the particle

B = ratio of amplitude to wavelength

B_{max} = maximum value of B

D = size of nanoparticle

D_{avg} = average size of nanoparticle

d = gap between two flat surfaces

E' = effective elastic modulus of surface and nanoparticle

F_{NP} = force on single nanoparticle

F_{ext} = external load/force applied to the surfaces

F_c = critical force

F_p = external force carried by the particles

F_s = force between surfaces

R = radius of nanoparticle

N_{NP} = numbers of nanoparticles in contact

S_y = surface yield strength

P' = average contact pressure

V_{NP} = wear volume instigated by nanoparticles

wt% = weight percentage of nanoparticle

σ_g = standard deviation of nanoparticle

a_v = void radius of the particle

ρ_{NP} = density of nanoparticle

ρ_{lub} = density of lubricant

τ_p = shear stress

ω = nanoparticle indentation

ω_c = critical indentation

φ = nanoparticle distribution

f_s = friction coefficient for asperities

B_c = critical value of B

μ_s = friction coefficient of asperities

μ_p = friction coefficient b/w particle & surfaces

v = Poisson ratio

E_{NP} = nanoparticle elastic modulus

E_S = surface elastic modulus

CHAPTER 1: INTRODUCTION

In modern era it is important to manipulate simplified version of equations that can help in predicting real area of contact b/w rough surfaces and that can be related to friction and wear. We are well aware of the fact that surfaces are rough on microscopic scale and this leads to the conclusion that nominal contact area is much larger than real contact area.it is very difficult to foretell real contact area between rough surface and how it varies with load.

1.1 Tribology

When two surfaces approach each other the most interacting phenomena occur is tribology. It is related to friction, wear, lubrication and energy losses. To control these energy losses, friction and wear should be improved [1]. To fulfill lubrication necessities, explicitly in modern aspect of tribology, the suitable approach is to choose a particular lubricant. Lubricant prevent surfaces to be in contact and thereby reduce friction [2]. It is not necessary that because of high lubricant in between rough surfaces, it comes out with better wear results. Three types of wear outcomes will occur when surface approach each other, their asperities comes in contact with each other are as follow fatigue, adhesion and abrasion [3].

1.2 Energy Losses

Energy losses will happen due to friction. It has been disclosed that energy losses in vehicle are 76-82%, engine losses is in range between 68-72% and losses that can occur due to friction is about 3% and are depicted in figure 1[4,5]. Total losses accounted due to friction and wear is about 30% [6]. To avoid these short of energy losses best lubricant should be used.

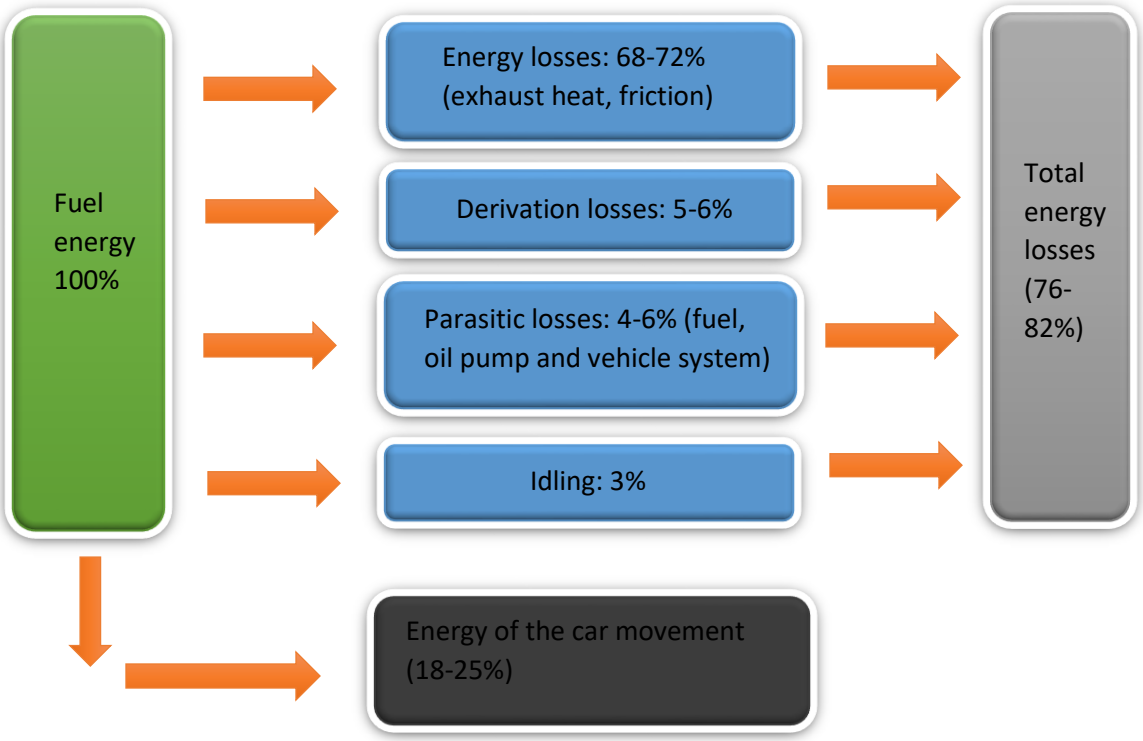

Figure 1.1: Energy losses in vehicle [4, 5].

1.3 Lubrication

Lubrication is an indispensable tool to reduce friction when two surfaces approach each other. There are three types of regimes. First one is Boundary lubrication regime, second one is mixed lubrication regime and third one is hydrodynamic lubrication regime [7]. Boundary lubrication takes place when thin tribofilm due to heavier load generates heat on the rubbing surfaces and this create high wear and energy losses. Thus, lubricant are incorporated in between rubbing surfaces to prevent from wear and friction [8]. Mixed lubrication regime will occur when slightly lower load as compare to boundary lubrication will apply on rubbing surfaces and this further shifted into hydrodynamic lubrication regime. Through this transition phase from mixed to hydrodynamic lubrication regime, thick layer of lubricating fluids are present in between rubbing surfaces and this will turn down friction and wear. In this hydrodynamic lubrication regime, except fatigue, no mechanical wear are present in between rubbing surfaces [8]. Rolling motion involved in elastohydrodynamic lubrication, otherwise it is much more similar to hydrodynamic lubrication

regime. ML regime is accumulation of BL and hydrodynamic lubrication regime. In mixed lubrication regime, tribofilm has 1-3 times greater film thickness than surface roughness. Tribofilm has three time's greater film thickness then surface roughness in hydrodynamic lubrication regime [9]. Tribofilm in elastohydrodynamic lubrication is very much small and as compared to hydrodynamic lubrication regime, greater pressure will be exerted on surfaces. In hydrodynamic lubrication regime, COF has value less than 0.01. In elastohydrodynamic lubrication regime, value of COF in ranges between 0.01 to 0.10 while in BL regime it will be greater than 0.1 [3].

Different lubrication regimes are demonstrated in stribeck curve, subjected to the ratio of lubricant film thickness to the roughness height.. Stribeck curve is divided into four sections, each section represents different lubrication regime as shown in figure 1.1a

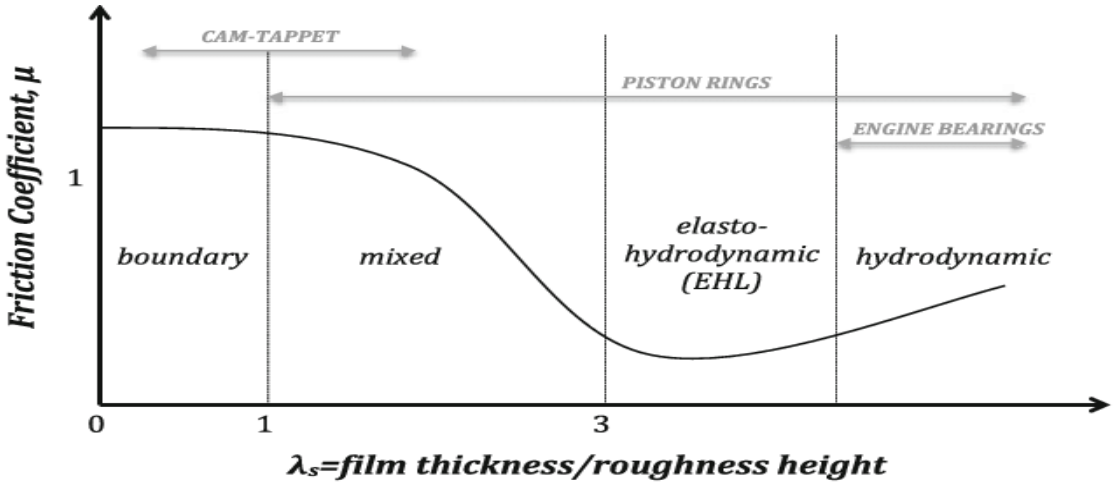

Figure 1.1a: Stribeck curve of different lubrication regimes [93]

1.4 Nanolubricants

Nanoparticles acts as lubricant additives are known as nanolubricants. Usually, they are in range between 1nm to 100nm. Remarkable amount of friction and wear could be reduced while implying nanolubricants on surfaces. Nanolubricants synthesis can be approach in two steps. In first step

through chemical process while in second step through physical or chemical method by applying nanoparticles in dry powder form. And in second step , dry nanoparticles are dispersed in lubricant with the help of surfactants [10].

1.5 Base Oils

On the basis of physical appearance, lubricants characterized into three forms: solid, semisolid and liquid form. Synthesis of three types of base oil are possible. These three types are: mineral oil, synthetic oil and biolubricant. American petroleum institute characterized base oil under the act of AP1 1509 as in table 1[11]. Group's I-III are refined from crude oil. Group IV are related to Polyalfaolefinoil (PAO) synthetic lubricants. Group V oils are not related to previous first four groups. This group comprises of organophosphates, polyalkyleneglycol (PAG), silicone and polyolester. * in table 1 belongs to mineral oil and ** belongs to synthetic oil category.

Characterization of Base oil	Properties		
	Sulfur Percentage	Saturates Percentage	V.I
Group 1(Solvent refined)*	> 0.03	< 90	78.8 to 119.8
Group 2(hydrotreated)*	< 0.03	> 90	78.8 to 119.8
Group 3(hydrocracked)*	< 0.03	>90	> 121
Group 4**	Related to Polyalfaolefin oil		
Group 5	All other base oil are not included in group I to IV		

Table 1: API oil characterization [11]

Fractional distillation is a process by which mineral oil is obtained. Mineral oil characterized into three groups: paraffinic, naphthenic and aromatic. Paraffin straight chain hydrocarbon include in paraffinic group, cyclic structure with no saturated bonds are included in naphthenic group and cyclic structure are included in aromatic [12, 13]. Mineral oil is very commonly used in industry but its effect on human health is very outrages. Minerals oil are commonly used in engine, gears and bearings.

The oil which usually made from hydrocarbon is synthetic oil. Synthetic oil has huge edge over mineral oil especially to provide lubricity in extreme high and low temperature and provide great resistance to wear [13]. Synthetic oil has great amount of benefits including improving energy efficiency, reduce maintenance cost and reduce energy consumption. Besides its huge benefits its demand in modern era will increased [14]. Some synthetic oil harms the environment [15].

Biolubricants possesses great amount of advantages as compared to mineral oil in many aspects like viscosity index of biolubricants are much higher than mineral oil, similarly high flash point and high dispersion [16, 17].

1.6 Types of Nanoparticles as Lubricant Additives

Nanoparticles can be characterized into different forms depending on their chemical composition: metal, metal oxide, nanocomposites, sulphides, carbon nanoparticles & rare earth compounds. Nanoparticles which consists of metals are mostly studied [18]. While the studies that have been carried out on rare earth compound and carbon nanoparticles are just 7%.

1.6.1 Metals

Metals nanoparticles are characterized on the basis of these properties which distinguish them from other nanoparticles are: low MP, high surface area and very minute particle size. They have exceptional tribological properties and their self-repairing function act as lubricant additives [19].Padgurskas et al. [20] incorporated Co, Cu and Fe nanoparticles in SAE 10 mineral oil. He delineated that Cu nanoparticles are most efficient in reducing both friction & wear in mineral oil and mixture of these three nanoparticles are also effective in mineral oil. Asadauskas et al. [21] incorporated Cu, Fe, and Zn nanoparticles in b/w mineral oil, synthetic oil and vegetable oil. They delineated that Fe nanoparticles have superior dispersion stability than Cu nanoparticles and Zn

nanoparticles. Wear resistance of rapeseed oil enhanced by Fe nanoparticles while Zn nanoparticles lesser wear.

When nano-bismuth particles are incorporated in heavy and light base oil it reduced the wear from 651 to 563 and 535 to 454 respectively. It also reduced friction from 0.074 to 0.047 and 0.091 to 0.052 respectively [22]. Addition of Ni nanoparticles in polyalfaolefin oil (PAO6) resulted in friction reduction of 5-45% and also wear reduction in ranges between 7-30% [23]. Moreover, Al nanoparticles enhanced wear and friction and improve load carrying capability [24]. Copper nanoparticles are incorporated in teboil ward results in reduction of friction from 0.15 to 0.1 [25]. Copper nanoparticles are added in SAE 15W40 base oil results in decrease in wear until nanoparticles concentration are increased in base oil [26]. Copper nanoparticles of diameter in range between 25-85nm are added in progamia base oil reduced both COF and wear but 1% increase in concentration of particle will results in both increase in wear and COF [27]. When tin and iron are incorporated into macs base oil results, result of this will reduce both friction and wear [28]. When copper nanoparticles are enumerated into lithium grease results in 82% wear loss and also results in 12% friction reduced [29].

1.6.2 Metal Oxides

Several types of metal oxides nanoparticles like ZnO, TiO2, CuO, Al2O3 acts as lubricant additives. Certain types of effects are similar in both metals and metals oxides nanoparticles: sintering effect, rolling effect, repair effect and rolling effect.

Alves et al. [30] included CuO and ZnO nanoparticles in synthetic oil & mineral oil and compare their tribological properties. They found that ZnO and CuO both nanoparticles are beneficial in terms of reducing friction & wear while the accumulation of both particles in vegetable oil is no fruitful in terms of wear reduction. Incorporation of TiO_2 nanoparticles in water based lubricants perform exceptional tribological properties [31, 32]. However addition of TiO_2 nanoparticles in SAE 20W40 proved to be significant in terms of both friction & wear reduction by 50.02% [33]. Luo et al. [34] investigated tribological properties of Al2O3 nanoparticles in thrust ring tribometer and four-ball tribometer. They found that friction decreased by 23.93% with the help of thrust ring tribometer while friction and wear reduced by four-ball tribometer are 17.62% and 41.76% respectively. Incorporation of Al2O3 nanoparticles in polyalfaolefin oil (PAO) and SAE 75W85

provided excellent results [35]. Incorporation of CuO nanoparticles in paraffin oil enhances tribological properties in terms of friction & wear [36]. Introduction of CuO nanoparticles in mineral oil decreased friction by 50% [37]. ZnAl2O4 nanoparticles incorporated in pure lubricant oil reduced both wear and friction by 31.2% and 33.67% respectively [38]. Copper oxide nanoparticles are added in palm kerned oil (PKO) reduced wear by 56% [39]. Incorporation of TiO_2 nanoparticles in oil in water proves to be significant reduction of friction by17.6% [40]. CuO nanoparticles are modeled in Polyalfaolefin oil which slightly improve friction but show promising result in wear, Hernandez Battez [89]. Alves [90] show the tribological properties of ZnO & CuO nanoparticles in synthetic & mineral oil.

1.6.3 Metal Sulphides

Several types of metal sulphide nanoparticles like MoS_2, WS_2, FeS, and CuS act as lubricant additives. Molybdenum disulhphide MoS_2 nanoparticles are superior in liquid lubricant as compared to micro Molybdenum disulhphide MoS_2 nanoparticles in terms of friction reduction [41].

Molybdenum disulhphide MoS_2 nanoparticles incorporated in dioctyl sebacate has improved the tribological properties in terms of friction & wear reduction than micro Molybdenum disulhphide MoS_2 nanoparticles because of the extra protective absorption layer on surfaces [42]. Inclusion of IF- MoS_2 and IF- WS_2 nanoparticles in polyalfaolefin oil (PAO) helped in reduction of friction and wear [43]. Gulzar et al. [44] incorporated MoS_2 and CuO nanoparticles in modified palm oil in which Molybdenum disulhphide MoS_2 show exceptional results than CuO nanoparticles in terms of friction and wear reduction. When FeS nanoparticles are added in engine oil lubricant additive, coefficient of friction would decreased effectively [45].

When Molybdenum disulhphide MoS_2 nanoparticles are incorporated in SE15W40, it improves the tribological properties of base oil [46]. Incorporation of WS_2 nanorod 2H- WS_2 in mineral oil display superior tribological properties than base oil [47]. Inclusion of Molybdenum disulhphide MoS_2 nanoparticles in coconut and paraffin oil shows that friction & wear would reduce with the rise of concentration until it reached the supreme concentration [48]. Incorporation of IF- MoS_2 in mixture of PAO4 and PAO40 has reduced maximum amount of friction from 0.2 % to 0.06% [49].

Addition of Multi-wall nanotubes MoS_2 nanoparticles in polyalfaolefin oil (PAO) has reduced the wear 5-9 times [50]

.

1.6.4 Carbon Based Nanoparticles

Various types of nanoparticles like diamond, graphene, and graphite act as lubricant additives. Peng et al. delineated that diamond nanoparticles in paraffin oil decrease the coefficient of friction because it provide suitable protection layer on contact surfaces [51]. When diamond nanoparticles are incorporated in polyalfaolefin oil (PAO) than tribological properties will change wear mechanism by converting adhesion to abrasion [52]. Gupta et al. [53] investigated tribological properties of graphite nanoparticles and delineated that it improves properties up to 18%.Sivakumar et al. [54] incorporated graphite oxide nanoparticles in waste carbon which show reduction in friction up to 21% & also reduce surface roughness up to 42.2%.

Graphene which usually called as "supermaterial" because it has exceptional physical, electrical and mechanical properties [55]. Inclusion of graphene in engine oil resulted in friction reduction up to 80% and wear reduction up to 33% and this is due to ball-bearing effect [56]. Lin et al. incorporated natural flake graphite and modified graphene platelets in SN350 base oil which shows that graphene exhibited excellent results [57]. Graphene by exfoliation should also be discussed [58, 59]. When graphite are incorporated in polyalfaolefin oil (PAO4) resulted in wear reduction by 80% and friction reduced from 0.2% to 0.12% [60].

1.6.5 Nanocomposites

There are many nanocomposites comprises of WC-Al_2O_3/graphene platelets, Cu/graphene oxide, TiO_2/SiO_2, Ag/graphene, graphite oxide/Cu, and Al_2O_3/TiO_2 which act as lubricant additives. Nanocomposites which have graphene should possess excellent tribological properties [61-63]. Tribological properties of WC-Al_2O_3/graphene platelets have been studied under 40N and 60N load condition. Coefficient of friction significantly reduced to 40.4% and 33.3% respectively under these two load conditions. Incorporation of graphene should lower abrasive wear [64].Inclusion of TiO_2/SiO_2 nanoparticles in palm TMP ester without the help of surfactant reduce friction and wear [65].

Accumulation of Cu- MoS_2 and Ag- MoS_2 nanoparticles decreased COF and enhance wear resistance [66]. Copper/carbon nanotube nanocomposite significantly lower down friction & wear

[67]. Incorporation of Cu- MoS_2 and Ag- MoS_2 nanoparticles in Litol and VNIINP grease helped in reduction of friction and essentially improve wear [68]. Hybrid Cu- Al_2O_3/Graphene platelets should decrease COF but as concentration of graphene is increased in mixture it created more wear in the surface [69]. Incorporation of Nano-Ag/MWCNTs particles in 10W40 engine oil reduced wear and friction up to 32.4% and 36.4% respectively [70].

1.6.6 Rare Earth Compounds

Rare earth compounds nanoparticles like LaF_3 and CeVO_4 acts as lubricant additives. The most important function of rare earth compounds are, they form tribofilm on interacting surfaces. La-doped Mg/Al nanoparticles incorporated in diesel engine oil CD 15W–40 show excellent tribological properties in term of friction reduction when particles form tribofilm on interacting surfaces [71].

Behavior of cerium oxide nanoparticles investigated that they perform excellent tribological properties in titanium and lithium grease [72, 73]. Inclusion of LaF_3 and CeVO_4 nanoparticles in fluoro silicone oil and liquid paraffin oil respectively shows exceptional tribological properties [74, 75].

1.7 Lubrication Mechanism of Nanoparticles

Nanoparticles reduced coefficient of friction and wear when they act as lubricant additives and they have ability to increase the load of mechanical parts. The most powerful factor which explain the tribological properties are lubrication mechanism of nanoparticles. Several effects which are incorporated in the study of lubrication mechanisms are: ball bearing effect, mending effect, protective film formation & polishing effect. These four effects are comprises of two groups: 1st group which can increase lubrication includes ball bearing effect & protective film formation, 2nd group which can increase surface properties include polishing and mending effect [76].

1.7.1 Ball Bearing Effect

Ball bearing effect which can also be characterized as rolling effect are in the form of spherical or quasi-spherical nanoparticles as shown in figure 1.2 that can roll and slide between two interacting surfaces and transform their sliding friction into rolling friction or rolling friction into sliding friction [51]. Viesca et al. [77] estimated that carbon coated nanoparticles enhanced tribological

properties when they appear in the form of ball bearing mechanisms. Raina and Anand [52] investigated tribological properties of diamond nanoparticles in the form of spherical shape to decrease the sliding contact and they are related to ball bearing mechanism.

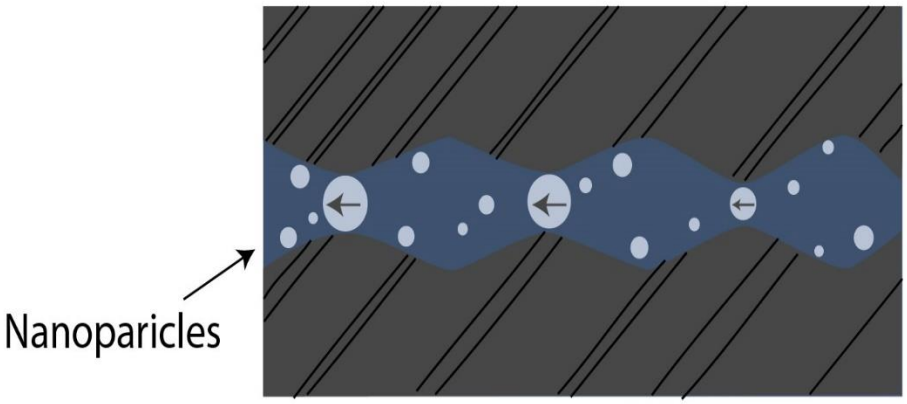

Figure 1.2: Rolling mechanism of nanoparticles in nanolubricant [94].

1.7.2 Protective Film Formation

As the name suggest, this effect describes the function of nanoparticles when they form protective layer on the surfaces which includes friction [51] as shown in figure 1.3. Meng et al. [71] delineated that surface roughness will reduce when silver nanoparticles form a protective layer on the surface. Protective film formation has vital role in reduction of friction parts by Wang et al. [78]. Various types of studies delineated about wear reduction [79, 80], friction and wear reduction [75] when protective films are applied on surfaces. Liu et al. [81] instigated the protective film strength. They relate strength and ductility with frequency. Ductility played a major role when frequency is greater and strength played a vital role when frequency is low.

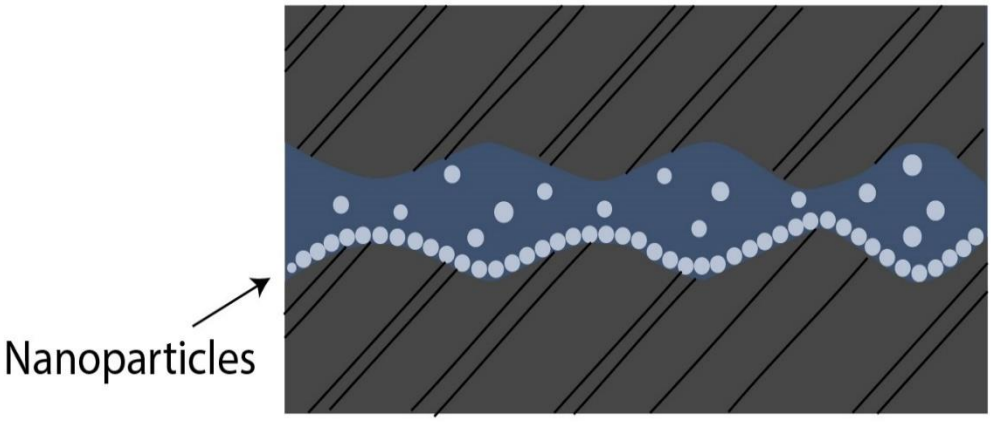

Figure 1.3: Nanoparticles protective film formation mechanism in nanolubricant [94].

1.7.3 Mending Effect

When nanoparticles are lay down on the interacting surfaces, it will compensate the loss of mass of asperities and due to this, it is designated as mending effect [51] as shown in figure 1.4. Yadgarov et al. [91] delineated that because of mending effect, wear occur on surfaces and this is due to IF-nanoparticles. Graphene/Ag nanocomposite nanoparticles enlightened self-repairing effect [62].

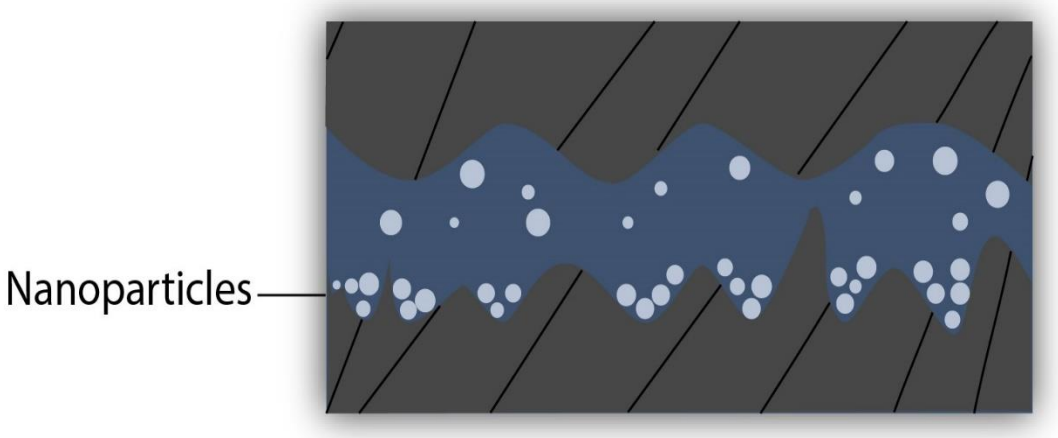

Figure 1.4: Nanoparticles mending effect mechanism in base lubricant [94].

1.7.4 Polishing effect

Another name given to this effect is smoothing effect because of the fact that it reduces surface roughness [76] as shown in figure 1.5. Ignole et al. [92] delineated that when TiO_2 nanoparticles are incorporated on the contacting surfaces, it create polishing effect on the surfaces because it depend on two phases: anatase and rutile phase. Wu et al. [32] investigated that friction surface defect removed by TiO_2 nanoparticles. Koshy et al.[48] reported that surface roughness could be reduced when nanoparticles fill the asperities.

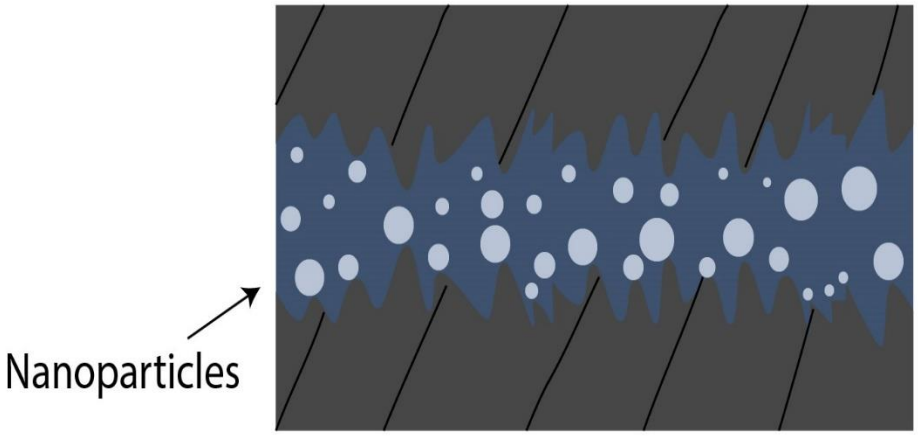

Figure 1.5: Nanoparticles polishing effect mechanism in nanolubricant [94].

CHAPTER 2: MODELING

This section described the full model in complete depth. This model is designated as multiscale model which is further segregated into two submodels, one refer to as rough surface contact model which consists of micrometer sized roughness features and second one refer to as statistical nanoparticle contact model which consists of nanosize particles.

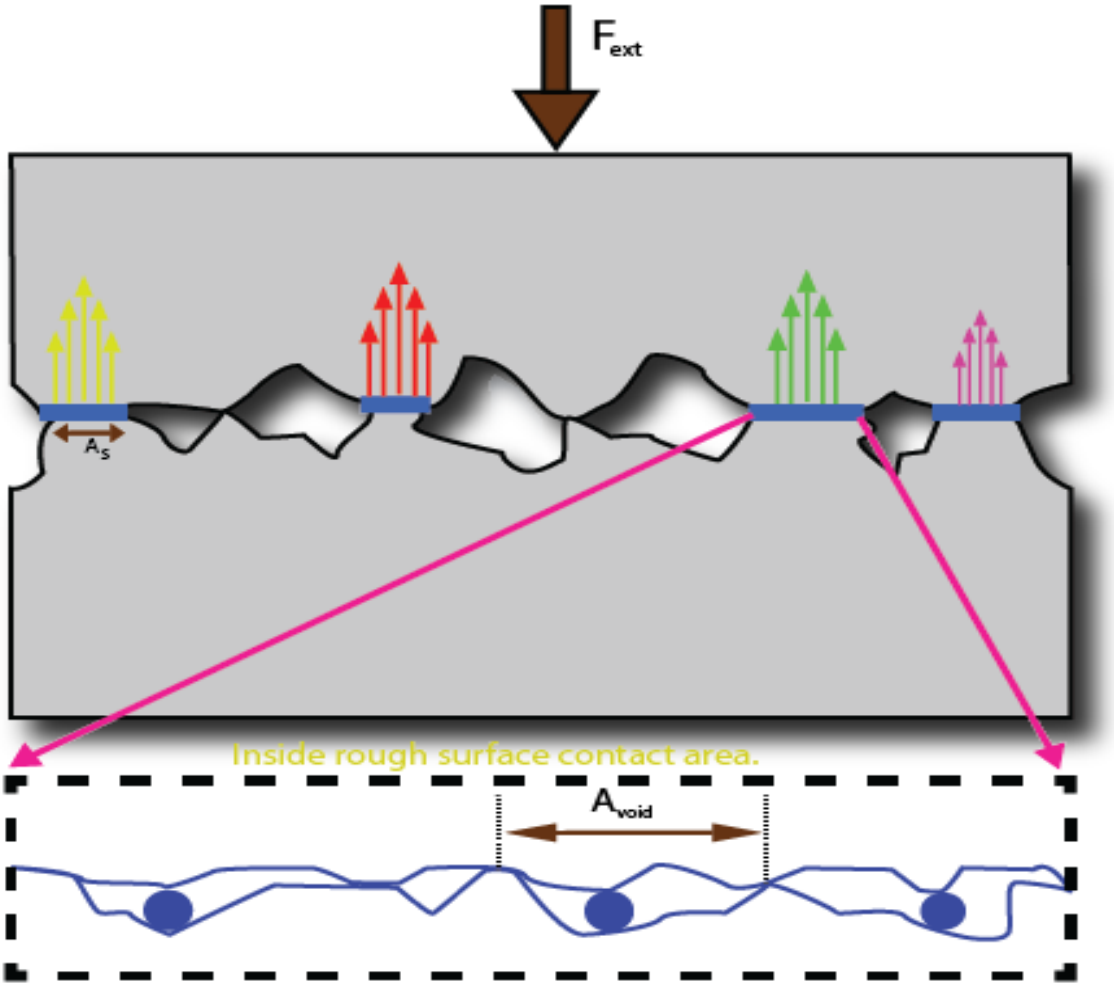

Figure 2.1: Demonstration of rough surface and statistical contact model

2.1 Rough Surface Contact Model

To find real contact area when two surfaces encounter, the first thing happen their asperities contact each other. Which leads to the result that some asperities deform elastically and some deform plastically. Surfaces are rough as a model suggest and with the help of FFT, bring down the surfaces into series of sine waves. Average contact pressure and contact area can be find from this model with the help of superposition. Certain parameters that are used in this model are, surface yield strength S_y , Poisson ratio v and B is amplitude to wavelength ratio.

$$P^* = \sqrt{2}\pi E' B_{max} \tag{2.1}$$

Equation (2.1) hold for elastic regime if

$$B_{max} < B_c$$

$$P^* = \sqrt{2}\pi E' B_{max} \left[\left(\frac{12\pi E' B_{max}}{\sqrt{2} S_y e^{\frac{2v}{3}}} + 7\right)/11\right]^{\frac{-3}{5}} \tag{2.2}$$

Equation (2.2) hold for plastic regime if

$$B_{max} > B_c$$

B_c is critical value of B

$$B_c = \frac{\sqrt{2}}{3\pi}\frac{S_y}{E'} e^{\frac{2v}{3}} \tag{2.3}$$

$$A_s = \frac{F_s}{P^*} \tag{2.4}$$

2.2 Statistical Contact Model

Many researchers had done work on contact between rough surfaces. To instigate this working on rough surfaces Greenwood [82] proposed their elastic contact model which is called GW model. The model consists of spherically shaped asperities with uniform radius of curvature and asperities height follow Gaussian distribution. To find real contact area & total load between rough & flat surface contact, elastic (Hertzian) assumption has been followed. To enlarge this basic GW model, Greenwood & Tripp [83] worked on contact between curved surfaces, asperities peak with varying radius of curvature Whitehouse & Archard [84], rumple asperities between two rough surfaces Greenwood & Tripp [85], elliptic paraboloidal asperities, Bush [86] and anisotropic surfaces, Bush [87]. Researchers had done enormous work on contact geometries but GW model presents exceptional results. But Greenwood & Williamson model can be imply to those conditions where asperities deform elastically and plasticity index should be low. Pullen [88] conducted experimental verification of GW model & model presents better results. However, the result straight away drift when applied load surpass yield load.

Contact between two nominally (apparent) surfaces, Greenwood and Williamson proposed their model regarding asperities contact. To model nanoparticles between two flat rough surfaces, statistical nanoparticle contact model is developed as shown in figure 2.2.

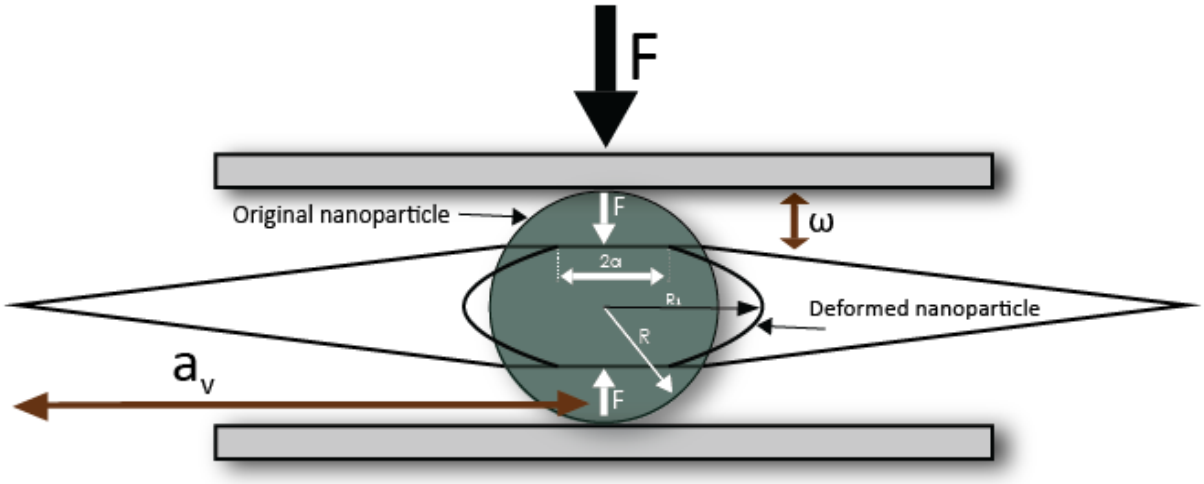

Figure 2.2: illustration of the spherical nanoparticle in contact between surfaces.

However revised certain parameters such as asperity density and height distribution and replaced with new parameters such as nanoparticle density and particle distribution respectively. From experimental results, particle density and Nano lubricant density can be figured it out. Nanolubricant density can also be found from this equation.

$$\rho_{\mathrm{sol}} = 100\left(\frac{wt\%}{\rho_{\mathrm{NP}}} + \frac{100-wt\%}{\rho_{\mathrm{lub}}}\right)^{-1} \tag{2.5}$$

To find out nanoparticle density in terms of separation equation (2.6) can be used

$$\eta(d) = \frac{\mathrm{N_{NP}}}{\mathrm{A_n}} = \left(\frac{\rho_{\mathrm{sol}}\, \mathrm{wt\%d}}{100\rho_{\mathrm{NP}}\left(\frac{\pi}{6}\int_0^{\infty} \varphi(D)D^3 dD\right)} \right) \tag{2.6}$$

For this model, particle distribution can assume as Gaussian function which can be described in terms of standard deviation.

$$\varphi(D) = \frac{1}{\sigma_g\sqrt{2\pi}} \exp\left[-0.5\left(\frac{\mathrm{D}-\mathrm{D_{avg}}}{\sigma_g}\right)^2\right] \tag{2.7}$$

Where D is the size of nanoparticle and σ_g is standard deviation of nanoparticle and D_{avg} is the average size of nanoparticle and φ is the distribution in terms of diameter.

As nanoparticle is modeled between two flat rough surfaces so apply external load F_{ext} to the surfaces it first deform the particle elastically on lower load and when apply greater load it deform the particle plastically. As in (Mook and Nowak 2007) some nanoparticles would deform and that percentage is 45% excluding others those that are being fractured. As in nanolubricant there are greater number of nanoparticles so for this case just model one nanoparticle. (Wadwalker 2010) developed the model of heavy loaded sphere and that model one presumption is that volume of heavy loaded sphere is constant.to find particle contact radius, equation are being displayed.

Jackson and Green 2010) presented their equation for particle contact radius. There are certain restriction related to those equation for which deformation case $a/R < 0.41$. But for plastic contact the criteria defined as $a/R = 0.41$.

$$\left(\frac{a}{R}\right) = \left(\frac{a}{R}\right)_1 + \mathrm{A_1}\left(\frac{\omega}{\omega_c}\right)^2 - \mathrm{A_2}\left(\frac{\omega}{\omega_c}\right) \tag{2.8}$$

$$A_1 = 0.0826\left(\frac{S_y}{E'}\right)^{3.148} \tag{2.9}$$

$$A_2 = 0.3805\left(\frac{S_y}{E'}\right)^{1.545} \tag{2.10}$$

$$\left(\frac{a}{R}\right)_1 = \sqrt{\frac{\omega}{R}}\left(\frac{\omega}{1.9\omega_c}\right)^{\frac{B}{2}} \tag{2.11}$$

This is modified form of Jackson and green equation that are being incorporated while evaluating particle contact radius.

$$B = 0.14\exp\left(23\frac{S_y}{E'}\right) \tag{2.12}$$

For the presumption of axi-symmetric contact, contact area for single nanoparticle can be found from this.

$$A_{NP} = \pi a^2 \tag{2.13}$$

Critical indentation can be described in equation (2.14)

$$\omega_c = \left(\frac{\pi c S_y}{2E'}\right)^2 R \tag{2.14}$$

$$C = 1.295\exp(0.73v) \tag{2.15}$$

$$\frac{F_{NP}}{F_c} = \left\{exp\left[-\frac{1}{4}\left(\frac{\omega}{\omega_c}\right)^{\frac{5}{12}}\right]\right\}\left(\frac{\omega}{\omega_c}\right)^{\frac{3}{2}} + \frac{P}{F_c}\pi R^2\left(\frac{a}{R}\right)^2\left\{1 - exp\left[-\frac{1}{25}\left(\frac{\omega}{\omega_c}\right)^{\frac{5}{9}}\right]\right\} \tag{2.16}$$

Force on single nanoparticle can be evaluated from equation (2.16)

$$\frac{P}{S_y} = 2.84 - 0.92\left[1 - cos\left(\pi\frac{a}{R_2}\right)\right] \tag{2.17}$$

$$R_2 = \sqrt{\frac{R^3}{0.76(R-\omega)} - \frac{a^2}{2}} \tag{2.18}$$

$$F_c = \frac{4}{3}\left(\frac{R}{E'}\right)^2 \left(\frac{c}{2}\pi S_y\right)^3 \tag{2.19}$$

Void area are produced when nanoparticle entangled between two flat surfaces. Each nanoparticle behave like nano-indentor. However different surfaces possess different scale properties with respect to their geometry. The experiment of (Ohmura and Tsuzaki 2001) affirmed that steel nano-hardness around 10GPA .Half space elastic model were used to find void area around nanoparticle by this equation $A_{void} = \pi a_v^2$. Revising all parameters and incorporate in original GW model to obtain the final form of this model.

$$\frac{A_p(d)}{A_n} = \int_d^\infty \eta(y)\,\varphi(y) A_{NP}(\omega, D)\,dD \tag{2.20}$$

$$\frac{F_p\,(d)}{E' A_n} = \int_d^\infty \eta(y)\,\varphi(y)\,\frac{F_{NP}(\omega,D)}{E'}\,dD \tag{2.21}$$

$$\frac{A_V\,(d)}{A_n} = \int_d^\infty \eta(y)\,\varphi(y) A_{void}(\omega, D)\,dD \tag{2.22}$$

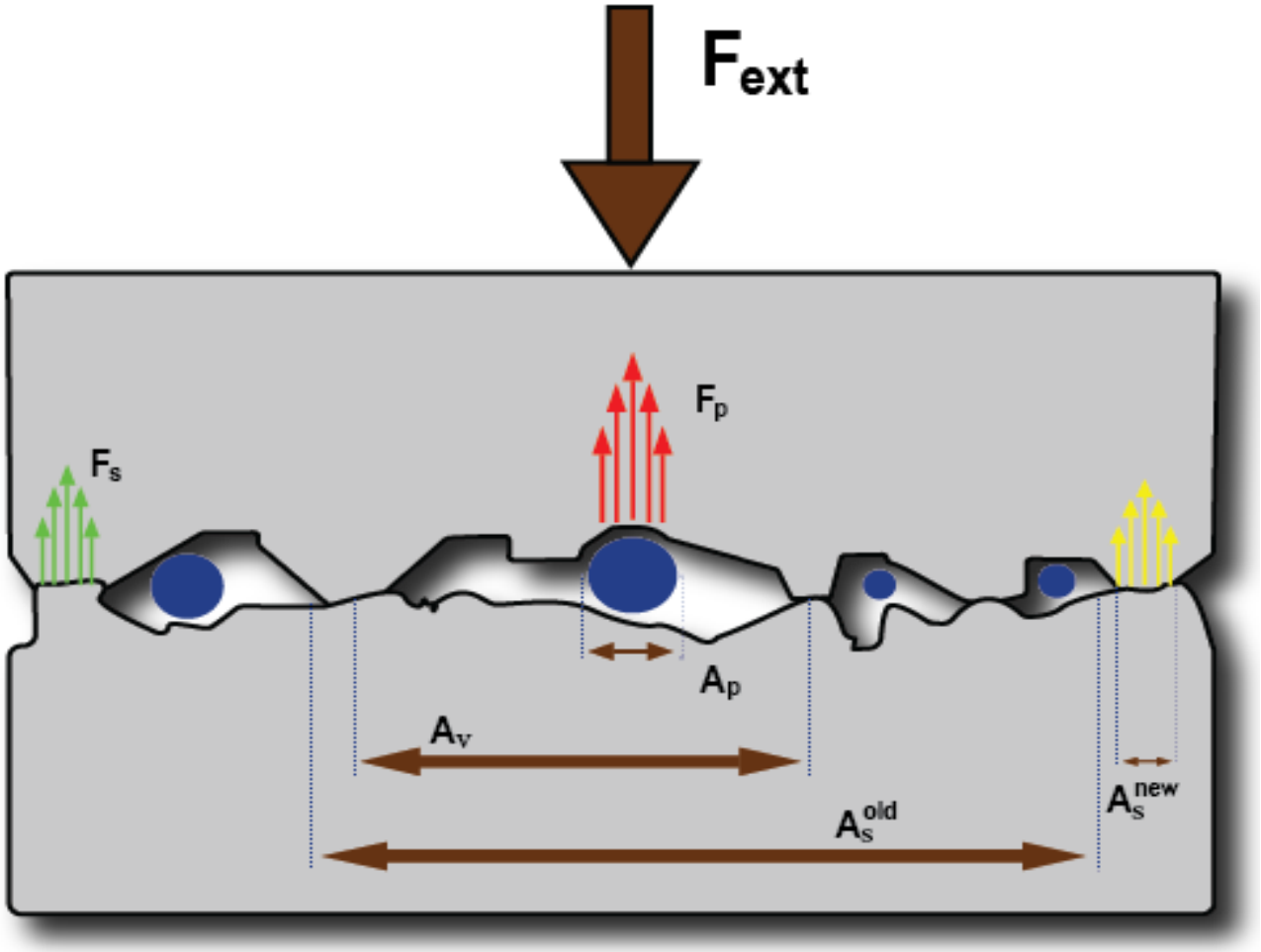

Figure 2.3: Illustration of overall nanoparticle contact phenomena

In above integral nanoparticle density η is function of separation. Interference can be described in terms of separation $\omega = y - d/2$ .The integral can be evaluated from composite Simpson method.

2.3 Algorithm

To solve the contact problem for two submodels an algorithm was developed. The main phenomena behind this algorithm is to check how much external load can surfaces bear and how much load can nanoparticle take and for this force balance equation is developed.

$$F_{ext} = F_s + F_p \tag{2.23}$$

First assume that surface can bear all the external load, then multiscale model should find average contact pressure and real contact area. Then also presume that same load is carried by the particle

$$F_p = A_S P \tag{2.24}$$

Then also assume that when surfaces are in contact, nanoparticles inside the flat rough surfaces also be in contact. Then conclude that A_S should be apparent contact area. Then surface area of contact should be updated as:

$$A_S{}^{new} = A_S{}^{old} + A_V \tag{2.25}$$

When surface area is updated it means surface force should also be updated

$$F_s = A_S P \tag{2.26}$$

Then from this equation $F_p = F_{ext} - F_s$ new updated force carried by particles can also be found. And then calculate the new values of A_V and A_p. Then again updating surface area and creating each loop again. Each loop convergence can be checked from this equation.

$$\left|\frac{(F_s{}^{new}-F_s{}^{old})}{F_s{}^{old}}\right| < 10^{-3} \tag{2.27}$$

To get final solution, this iteration is repeating again to ensure it meets the convergence criteria.

(Gelink and Schipper 2000) proposed that asperities friction coefficient has constant value. (Masjedi and Khansari 2014) concluded that friction coefficient of asperities ranging from 0.1 to 0.13.hence we obtained asperities friction coefficient from this relation.

$$\mu_s = \frac{F_{f,asp}}{F_{ext}} = \frac{F_s f_s}{F_{ext}} \tag{2.28}$$

$F_{f,asp}$ stands for friction force of lubricating surface. This value can be presume as 0.12 COF between nanoparticles and surface can be demonstrated with regard to this relation.

$$\mu_p = \frac{A_p \tau_P}{F_{ext}} \tag{2.29}$$

If check the nanoparticle hardness, then shear stress is presumed as 1.67GPa (Ohmura *et al.* 2001).to calculate friction coefficient this relation can be used

$$\mu = \frac{F_s f_s + A_p \tau_P}{F_{ext}} \tag{2.30}$$

To find wear model while amalgamating nanoparticles and surfaces is quite hard job. However based on statistical data one can find wear from (Williams 2005) model. From William model wear is proportional to interference cross-sectional area.

$$\frac{V_{NP}}{L} = \int_d^{\infty} \eta(y)\, \varphi(y) A_{CS}(\omega, D) dD \tag{2.31}$$

$$A_{CS} = \frac{D^2}{8}\left\{\sin^{-1}\left[\frac{8\omega(D-\omega)(D-2\omega)}{D^3}\right] - \frac{8\omega(D-\omega)(D-2\omega)}{D^3}\right\} \tag{2.32}$$

.

2.4 Contact Model

Suppose we have to characterize certain parameters that depend on particles that are in between rough surfaces. Also suppose total number of particles whose total mass is represented by M_p are scattered on the surface whose total area is represented by A_n, Hence mass density of the particles is represented by formula

$$m_p = \frac{\mathrm{M_p}}{\mathrm{A_n}} \tag{2.33}$$

Assume that particles possess certain distribution which is represented by $\emptyset_{\mathrm{P}}(D)$ where D is known to be particle size. Now, areal volume density can be represented by this equation.

$$\mathrm{v_p} = \frac{\mathrm{N_p}\pi}{6\mathrm{A_n}} \int_0^\infty \varphi_p(D)\, D^3 dD \tag{2.34}$$

Where $\mathrm{N_p}$ is accumulative number of particles in between rough surfaces. v_p can also be find from particle density.

$$\mathrm{V}_p = \frac{\mathrm{m}_p}{\rho_p} \tag{2.35}$$

Comparing equation (2.34) and (2.35), to find particles per area in equation (2.36)

$$\eta_p = \frac{\mathrm{N_p}}{\mathrm{A}_n} = \frac{6m_p}{\pi\rho_p}\left(\int_0^\infty \phi_p(D) D^3\, dD\right)^{-1} \tag{2.36}$$

Many contact models can be developed in stint of surface separation.

If we have to interpret surface separation, then assume that flat surface is in contact with rough surface. Then surface separation is the distance between rough surface to rigid flat surface. Let's assume that rough surface have height distribution that is $\phi_s(y)$. Let's also presume that rough surface is isentropic and its profile is elaborated as y = y(x). For contact model, two regions have been elucidated on surface separation. Region 1 have position which is defined as $y \geq d$ and region 2 is defined as $y < d$. When these two surfaces are in contact, their particles and asperities come contact with each other. Therefore accumulative effect of area of contact and overall contact force is defined in equation (2.37).

$$\frac{\mathrm{F}^1(d)}{\mathrm{E}'\mathrm{A}_n} = \int_d^\infty \eta_s \phi_s(y) \frac{\mathrm{F}_{asp}(\omega)}{\mathrm{E}'} dy + \int_0^\infty \eta_p(d) \phi_p(y') \frac{\mathrm{F}_p(\omega',\ y')}{\mathrm{E}'} dy'$$

$$\frac{\mathrm{A}_r(d)}{\mathrm{A}_n} = \int_d^\infty \eta_s \phi_s(y) \mathrm{A}_{asp}(\omega) dy$$

$$\frac{\mathrm{A}_p(d)}{\mathrm{A}_n} = \int_0^\infty \eta_p(d) \phi_p(y') \mathrm{A}_p(\omega',\ y') dy' \qquad (2.37)$$

In the above equation η_s represents areal asperity density. F_{asp} Represents single asperity force and A_{asp} represents single asperity area. F_p Represents single particle force. ω' Represents particle indentation.

In region 1, areal particle density can be defined as

$$\eta_p{}^1\,(\mathrm{d}) = \eta_p \int_d^\infty \phi_s(y) dy \qquad (2.38)$$

In equation (2.38), the 1st integral evaluates the overall effect of single asperity and 2nd integral evaluates the effect of particles and also A_p is not accumulated in A_r in region 1.

Region 2 is entirely complex as compared to region 1 because it includes those particles that are in contact. Equation (2.39) evaluates ${\eta_p}^2$, areal density of particles residing on surfaces at $y = y''$ in stint of surface separation d. $N_p * \phi_s(y'')$ is number of particles residing at the height $y = y''$. Larger particles are in contact when they fill this criteria $d - y''$. Number of particles are described in this equation (2.39)

$$N_p \phi_s(y'') \int_{d-y}^{\infty} \phi_p(q) dq \tag{2.39}$$

When equation (2.39) is divided by A_n

$${\eta_p}^2(d, y'') = \eta_p \phi_s(y'') \int_{d-y}^{\infty} \phi_p(q) dq \tag{2.40}$$

Now to discover average contact force & contact area in region II. Those particles which are in contact are of separate size. Thus average force & contact area can be calculated by this equation (2.41)

$$\frac{F_{avg}^2(d, y'')}{E'} = \left(\int_{d-y''}^{\infty} \phi_p(q) \frac{F_p(\omega'', q)}{E'} dq \right) \left(\int_{d-y''}^{\infty} \phi_p(q) dq \right)^{-1}$$

$$A_{avg}^2(d, y'') = \left(\int_{d-y''}^{\infty} \phi_p(q) A_p(\omega'', q) dq \right) \left(\int_{d-y''}^{\infty} \phi_p(q) dq \right)^{-1}$$

(2.41)

In equation (2.42), ω'' is the particle indentation and is represented by this equation (2.42)

$$\omega'' = \frac{[q-(d-y'')]}{2} \tag{2.42}$$

The force & real contact area can calculated by integrating over y'' in equation (2.43)

$$\frac{\mathrm{F}^2(d)}{\mathrm{E}'\mathrm{A}_n} = \int_{-\infty}^{d} {\eta_p}^2 \frac{\mathrm{F}_{avg}^2}{\mathrm{E}'} dy'' = \int_{-\infty}^{d} \left[\eta_\mathrm{p} \phi_s(y'') \left(\int_{d-y''}^{\infty} \phi_p(q) \frac{\mathrm{F}_p(\omega'',\ q)}{\mathrm{E}'} dq \right) \right] dy''$$

$$\frac{\mathrm{A}_r^2(d)}{\mathrm{A}_n} = \int_{-\infty}^{d} {\eta_p}^2 \mathrm{A}_{avg}^2 dy'' = \int_{-\infty}^{d} \left[\eta_\mathrm{p} \phi_s(y'') \left(\int_{d-y''}^{\infty} \phi_p(q) \mathrm{A}_p(\omega'',\ q) dq \right) \right] dy''$$

(2.43)

The contact model presented in this section can be implemented in various practical application.

CHAPTER 3: VALIDATION

This section describes the validation of model.

Figure 3.1a shows how particle induced wear vary with nanoparticle volume percentage. Silicon nanoparticles having density 0.773g/cc are suspended in conventional lubricant having density 2.329g/cc. As volume percentage of silicon nanoparticles increases, it increases particle induced wear per sliding distance. Particle induced wear drops to zero as nanoparticle concentration approaches zero which is due to fact that conventional surfaces are not included here.

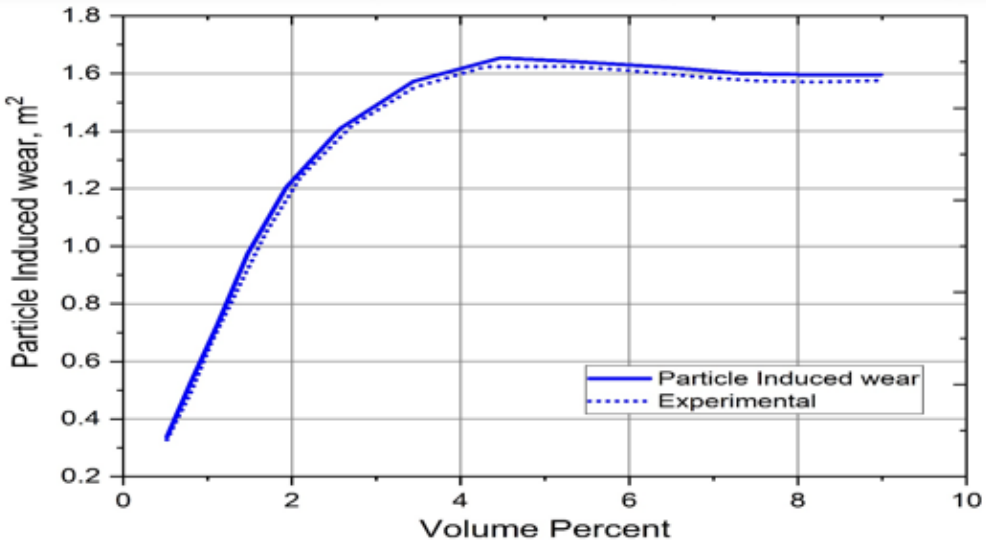

Figure 3.1a: Shows the result of particle induced wear versus volume percent of nanoparticles. Solid line shows the current work while dotted line shows experimental result.

Figure 3.1b shows how coefficient of friction vary with nanoparticle volume percentage. An increase in the content of nanoparticles decreases friction. This happen when real area of contact is reduced. As particle concentration increases, more particles engaged in a contact, than the average particle force decrease which will cease the contact.

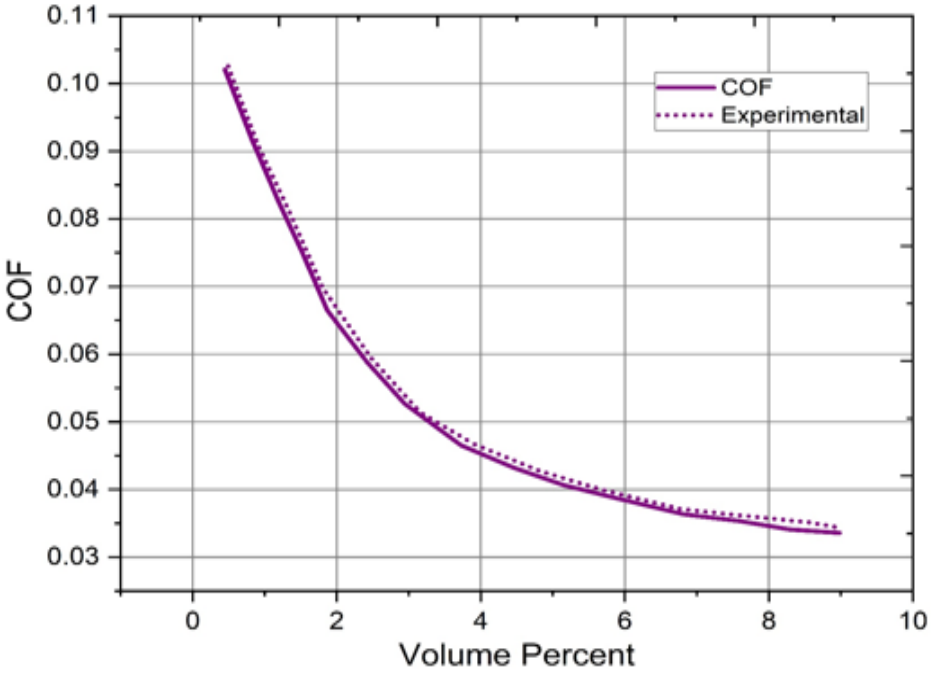

Figure 3.1b: Shows the result of coefficient of friction versus volume percent of nanoparticles. Solid line shows the current work while dotted line shows experimental result.

CHAPTER 3: RESULTS

This section describes the results of the model in complete depth.

Figure 3.1 show how coefficient of friction vary with particle volume percentage. It shows that as volume of nanoparticles increases, it decrease coefficient of friction. This in turn reduce the real contact area. This is happen when standard deviation of particle is $\sigma_g = 1.5nm$ and surface roughness is $0.05\mu m$. Figure 3.2 show how volumetric wear per sliding distance vary with particle volume percentage. As volume percentage of nanoparticle increase it enlarges volumetric wear per sliding distance. Volumetric wear per sliding distance will reduce if there is less nanoparticles in the mixture.

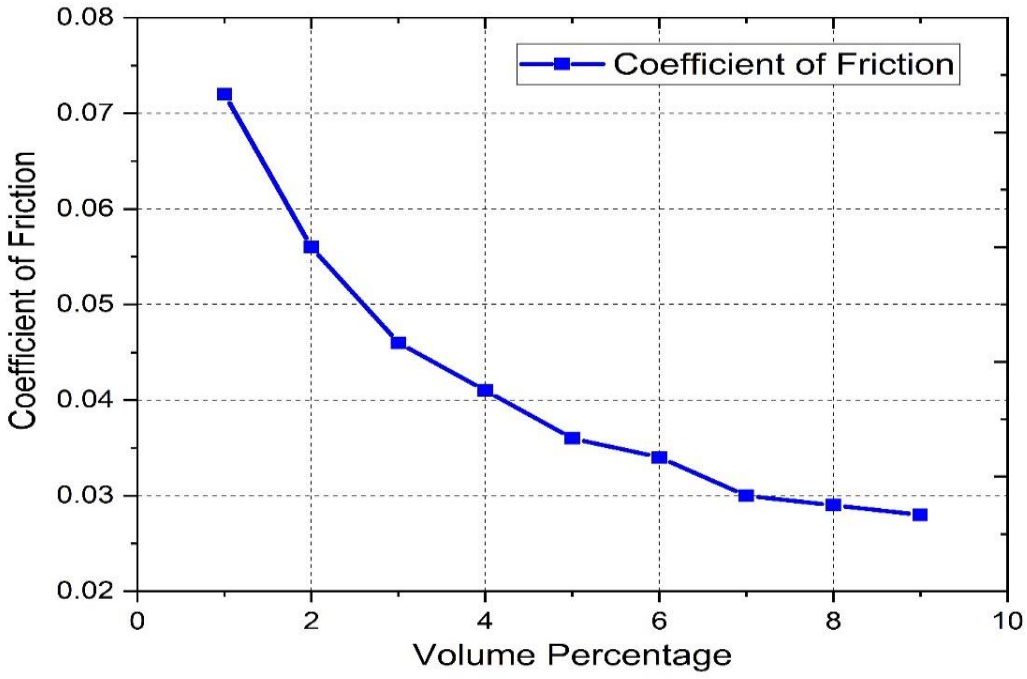

Figure 3.1: Coefficient of friction versus nanoparticle content

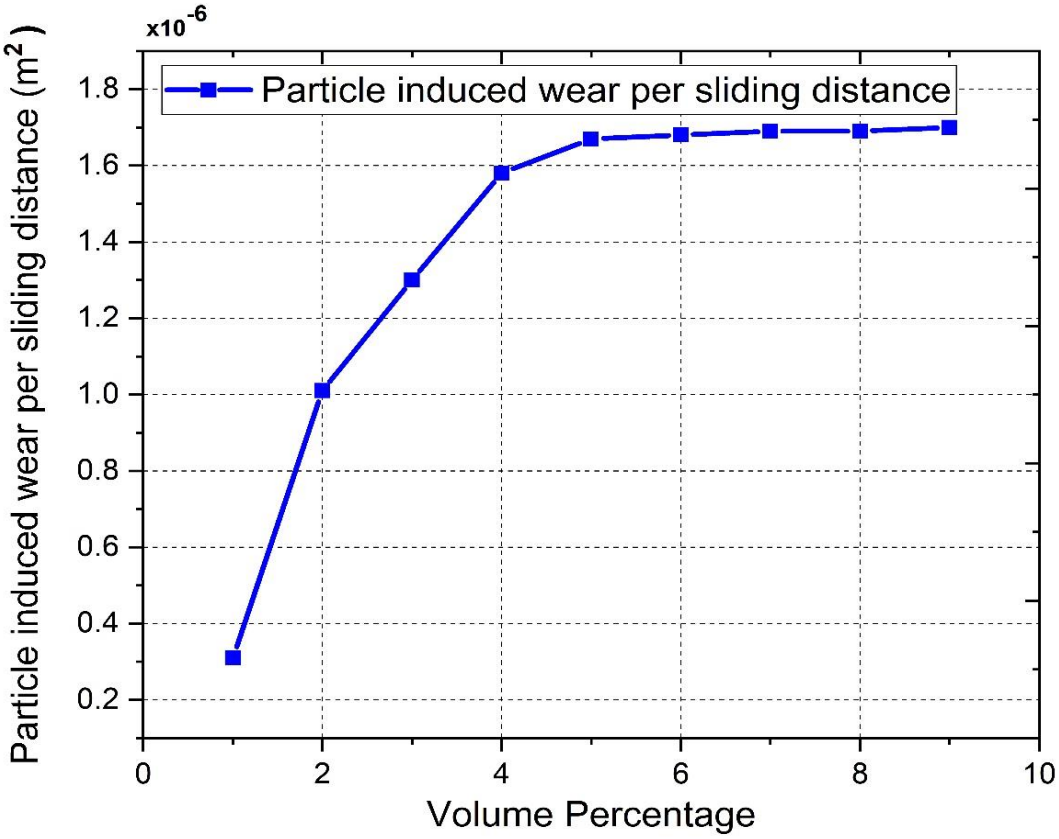

Figure 3.2: Particle induced wear versus nanoparticle content

Figure 3.3 shows how particle induced wear vary with nanoparticle size. Particle induced wear will be more as size of nanoparticle is smaller and particle induce wear is small as size of nanoparticle increase. So deduce a result from this, wear is inversely proportional to nanoparticle size. Which mean wear will be more as particle size is smaller and wear will be less as particle size increase. Figure 3.4 show how coefficient of friction vary with nanoparticle size. Coefficient of friction will reduce as size of nanoparticle is smaller and it enlarges as size of nanoparticle increases. Which mean coefficient of friction will vary directly with nanoparticle size.

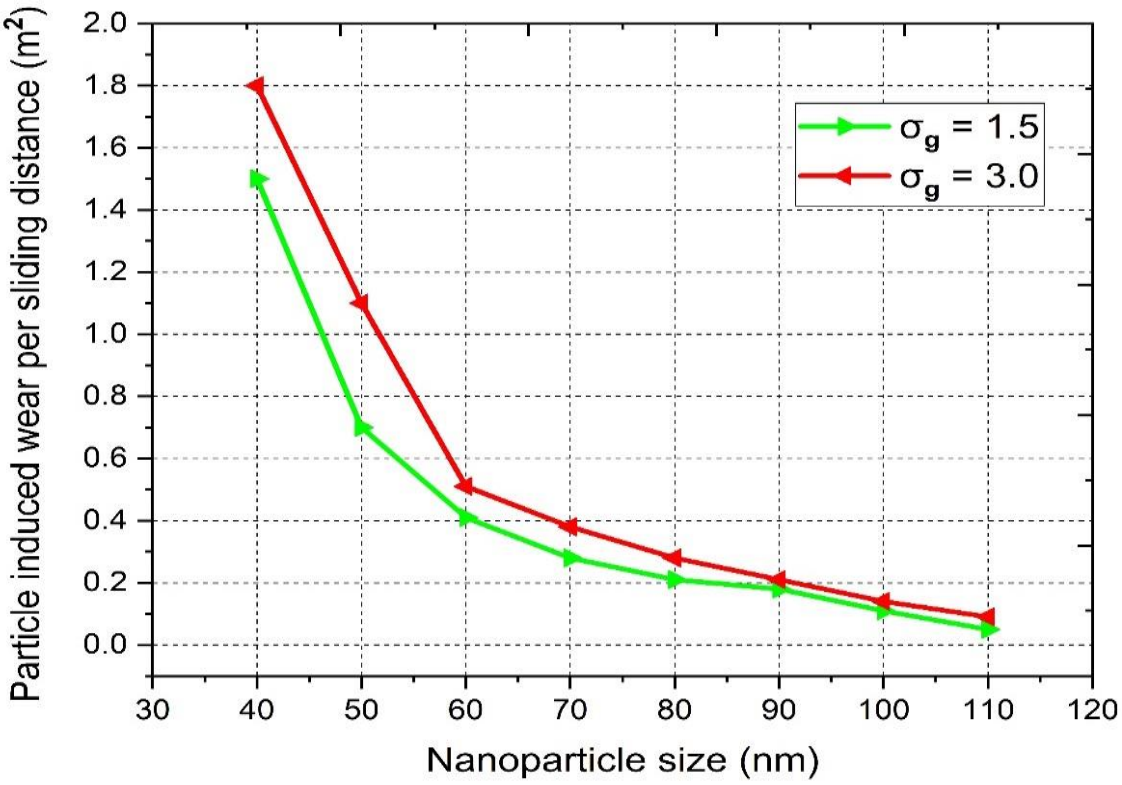

Figure 3.3: Particle induced wear changing with nanoparticle size

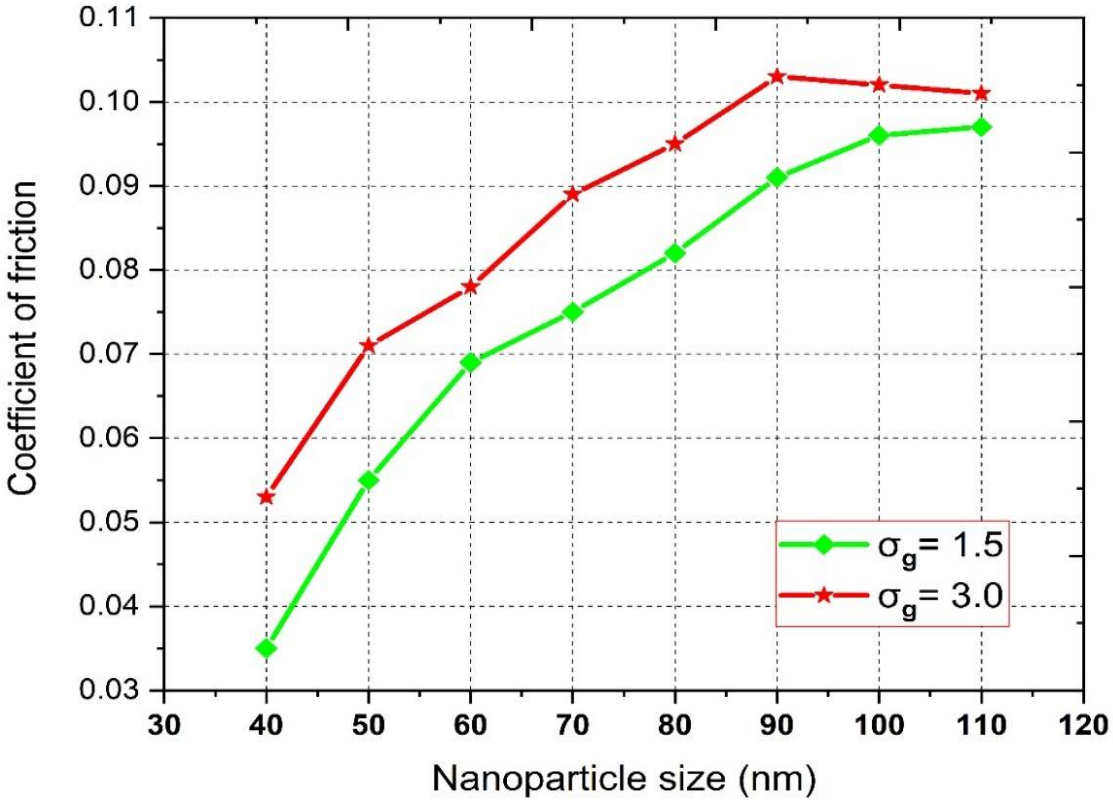

Figure 3.4: COF versus nanoparticle size

Figure 3.5 show the impact of particle concentration on dimensionless real area of contact and dimensionless pressure. Real contact area which is the accumulation of particle area and surface area. As volume percentage of nanoparticles enlarges, more nanoparticles are in contact and this reduce the real contact area and when percentage of nanoparticles reduced in the mixture it will increase the real contact area. In both cases, because of the introduction of nanoparticles in rough surface, it separates the surface apart which in turn reduce the real contact area.

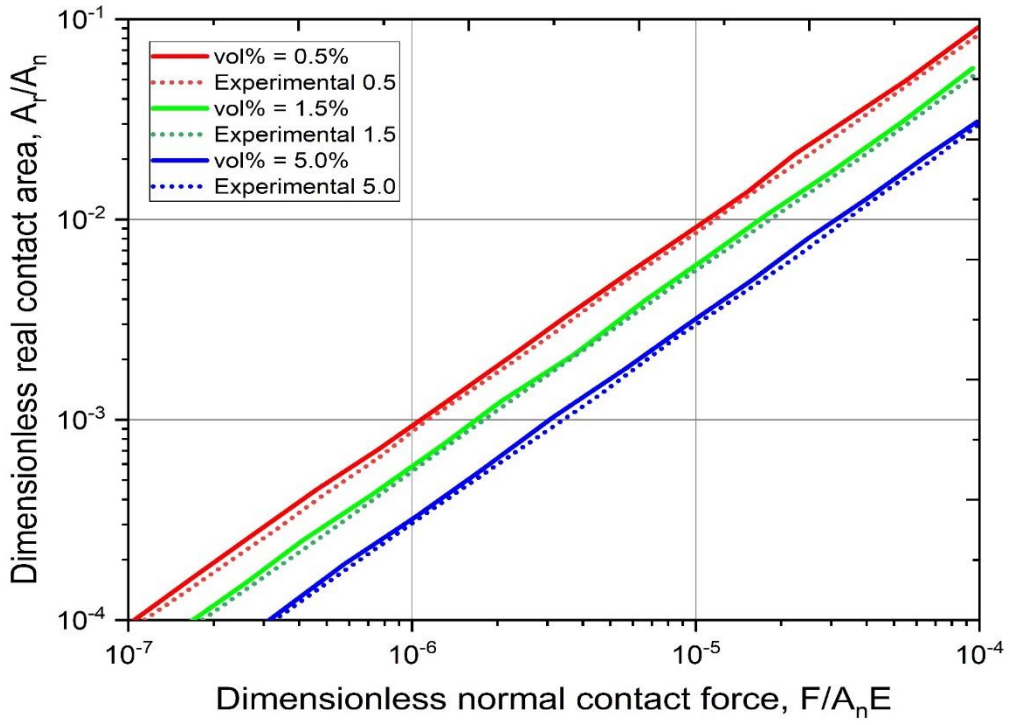

Figure 3.5: Figure shows the result of dimensionless real contact area versus dimensionless real contact force at different volume percentages of nanoparticles. Solid line shows the current work while dotted line shows experimental result.

Effect of particle distribution shown in figure 3.6. Different distribution are presented in the graphs that will impact on real area of contact and contact pressure. In the figure real contact area will reduce when approach to sharper peak. Wider distribution of particles bring into the rough surfaces contact and tend to become fracture.

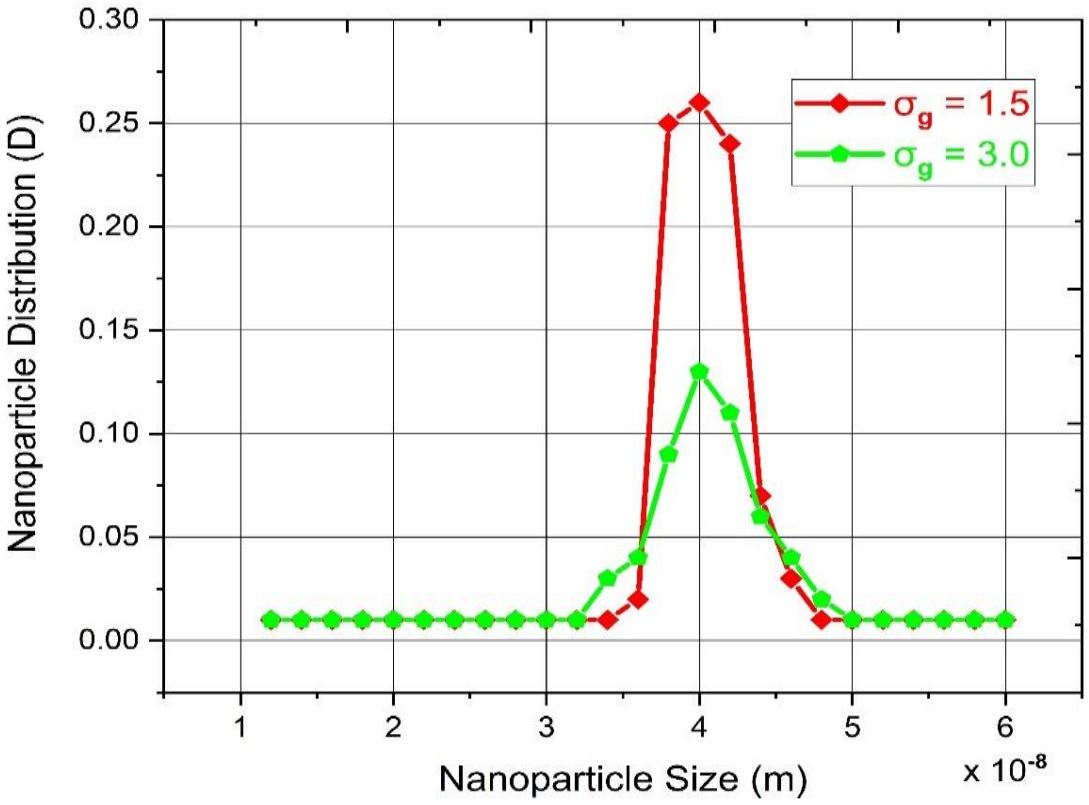

Figure 3.6: The impact of nanoparticle distribution on the real contact areas

Figure 3.7 show variation of fracture nanoparticles versus surface separation. Particles will tend to go less fractures if there are more surface separation and will tend to go high fracture if there is less surface separation.

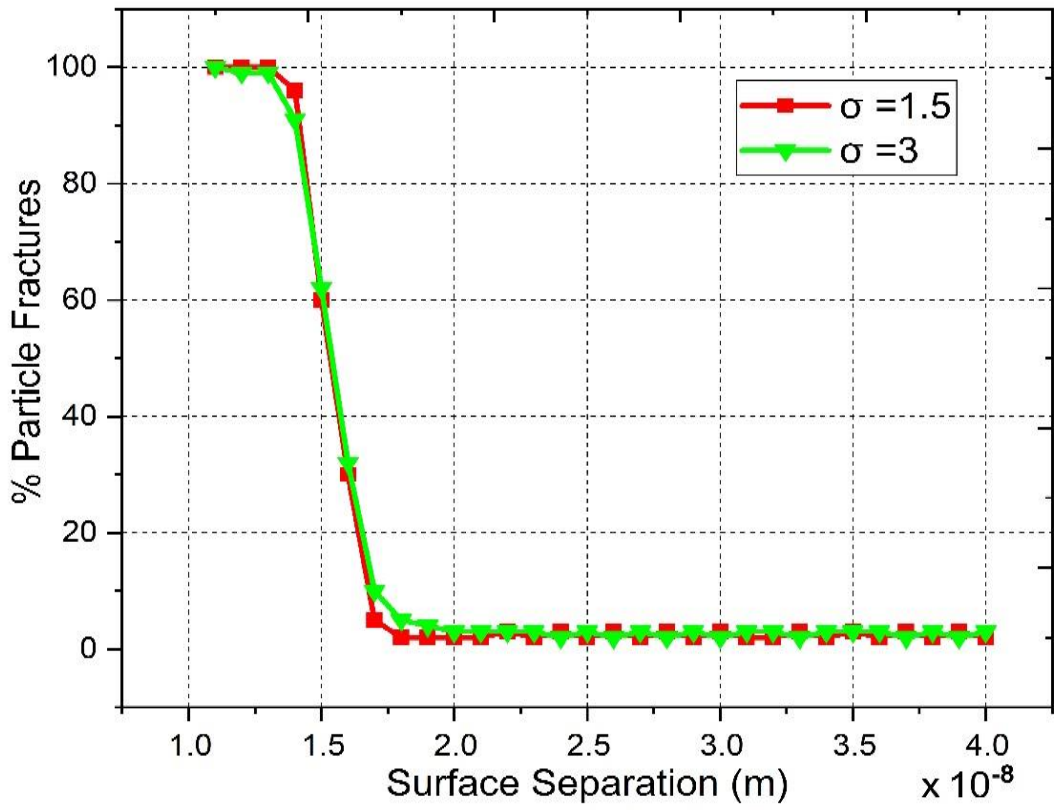

Figure 3.7: Nanoparticles fractured in terms of surface separation

Figure 3.8 show the comparison of the results between current model and experimental developed model.

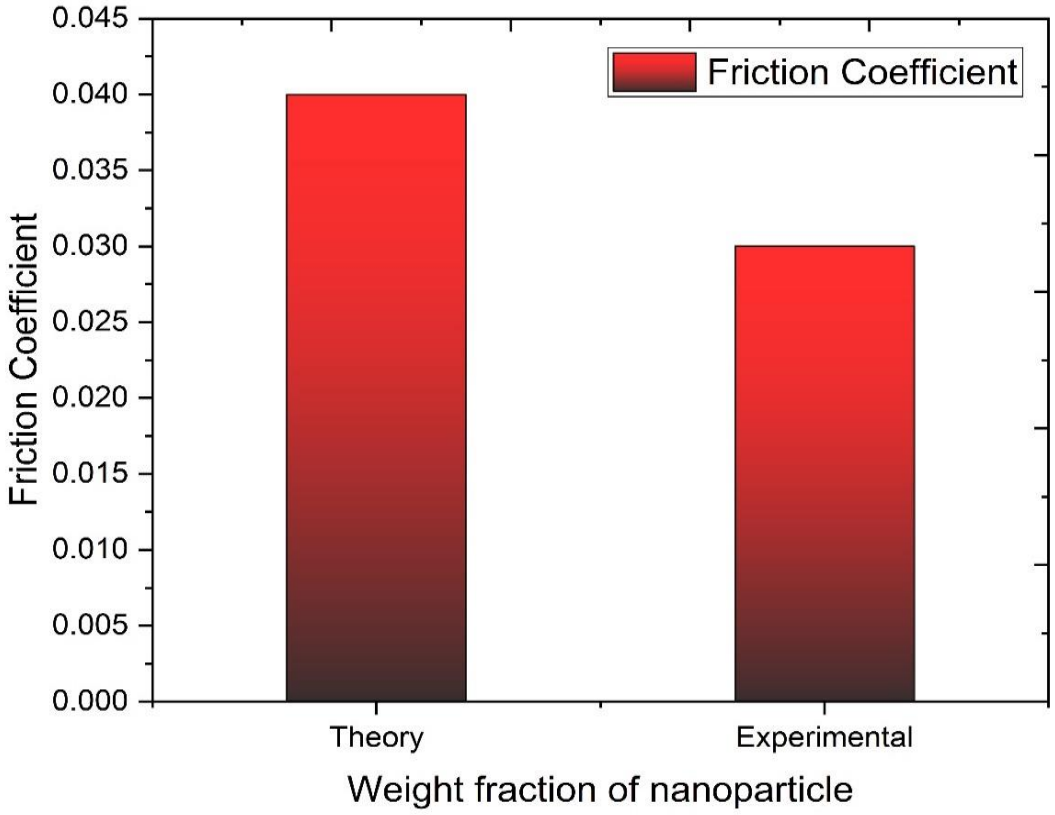

Figure 3.8: Comparison b/w experimental & numerical results for volume percentage of 5%

In Figure 3.9 when contact pressure are too much high because of insertion of more nanoparticles in the system, it reduces coefficient of friction. Because of high contact pressure, more asperities began to contact with each other and it yielded because of plastic deformation occur. Figure 3.9 shows that coefficient of friction decrease in boundary lubrication regime.

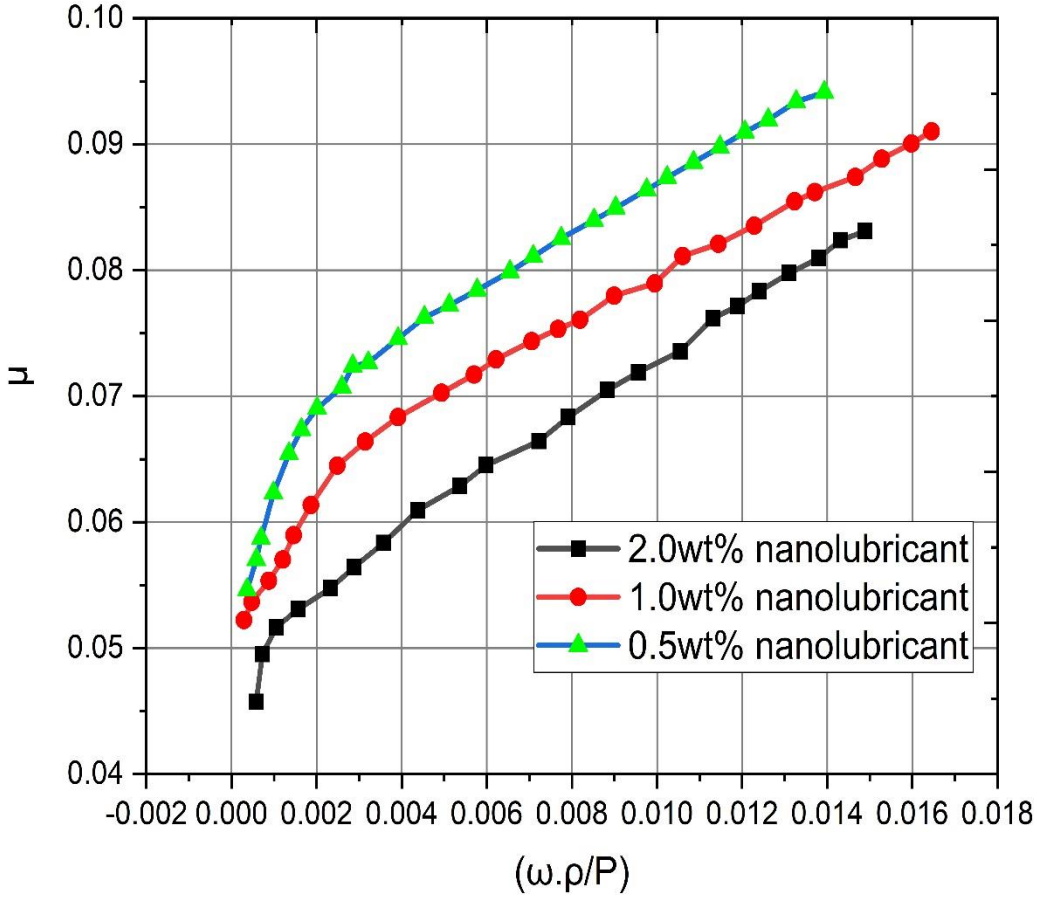

Figure 3.9: different weight fraction of nanoparticles

Figure 3.10 shows volumetric wear rate per sliding distance versus nanoparticle concentration. “V” speaks for volumetric wear rate while “s” shows sliding distance. Results indicate that wear escalate up to 1% weight concentration and wear reduces as particle concentration goes to 2%. Therefore, wear is larger at 1% and smaller at 2% weight fraction. This shows that addition of nanolubricant escalates wear in some cases while in other cases it enlarges.

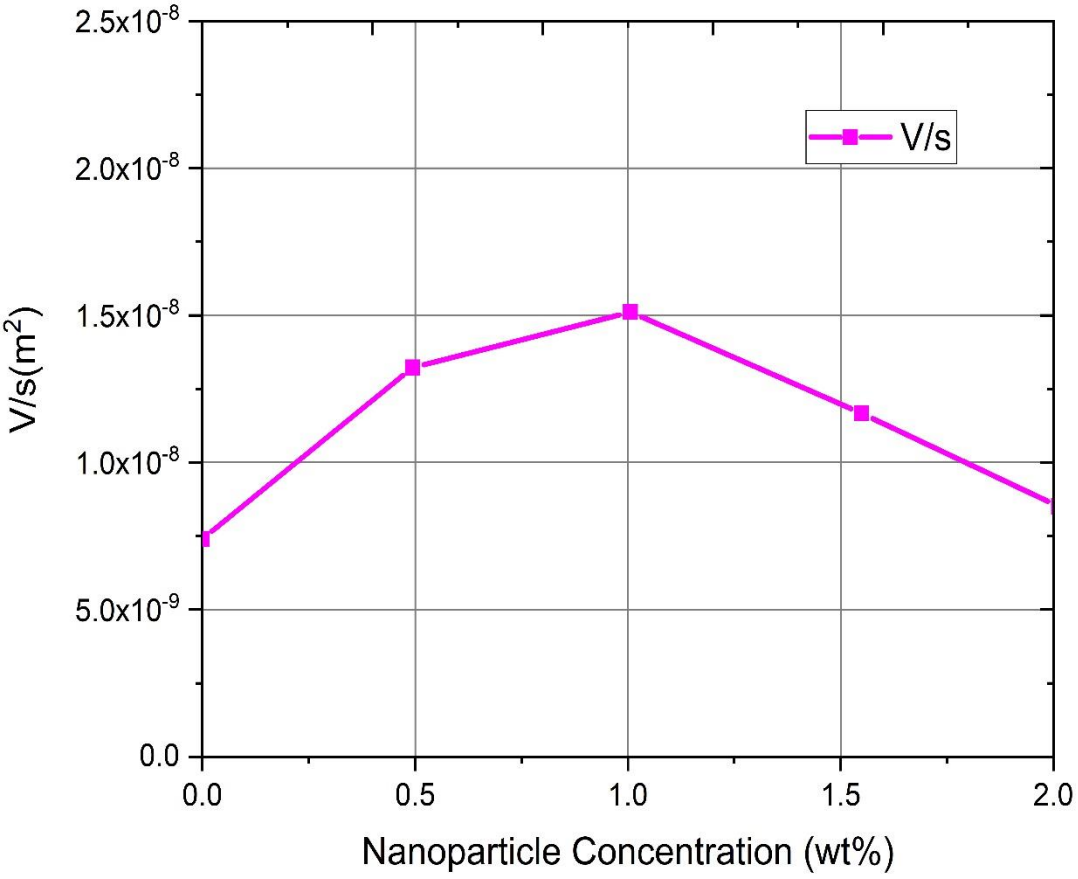

Figure 3.10: Nanoparticle concentration versus wear rate

Figure 3.11 displayed the results of base lubricant versus nanolubricant. As contact pressure escalates, coefficient of friction first reduces and then enhance which is common phenomena in this regime. When contact pressure are in range between 0.8 to 1.6 GPa, nanoparticles increase friction which is associated with this contact pressure. Viscosity of nanolubricant is higher than base lubricant. And when contact pressure is higher, lubricant squeeze out in between rough surfaces.

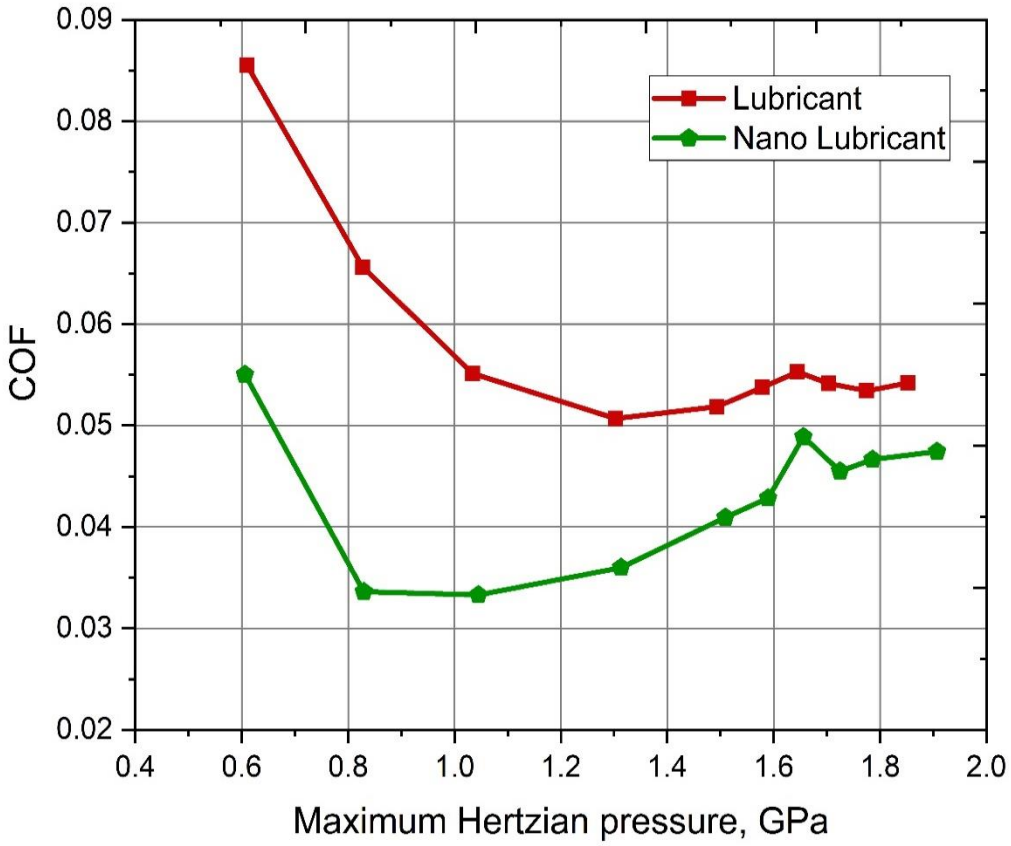

Figure 3.11: Coefficient of friction versus maximum hertzian contact pressure

Figure 3.12 shows that COF vary with sliding distance when distinct concentration of nanoparticles are inserted in between surfaces. Individual curve constitutes a coefficient of friction signal of a test. Figure 3.12 displayed that coefficient of friction in one step takes sliding distance of less than 1000 m because molybdenum disulphide nanoparticles are capable of maintaining friction.

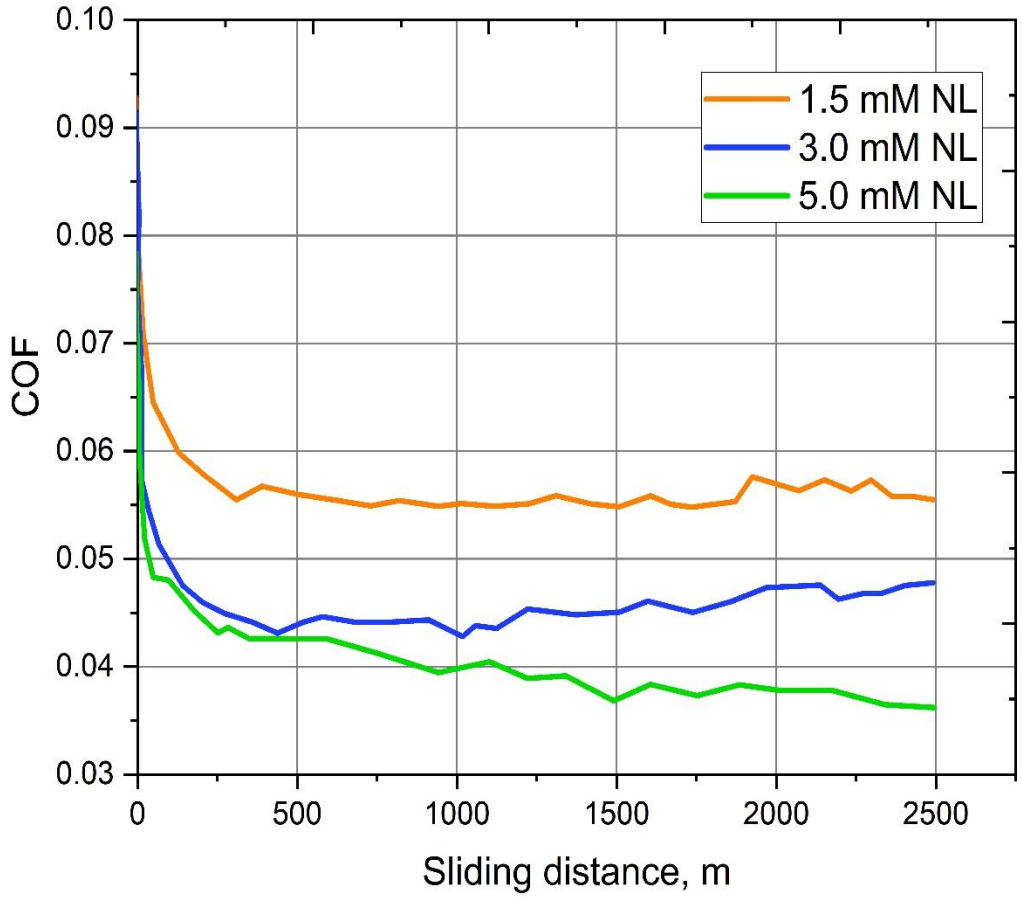

Figure 3.12: COF versus sliding distance of distinct concentration of nanoparticles

Figure 3.13 shows the results of COF versus nanoparticle concentration. As shown in the graph when particle concentration enhanced from 0 to 1, COF decreased from 0.070 to 0.060. And when particle concentration further increased from 1 to 2, COF decreased from 0.060 to 0.055 and same trend goes in this manner until coefficient of friction decreased to 0.040.

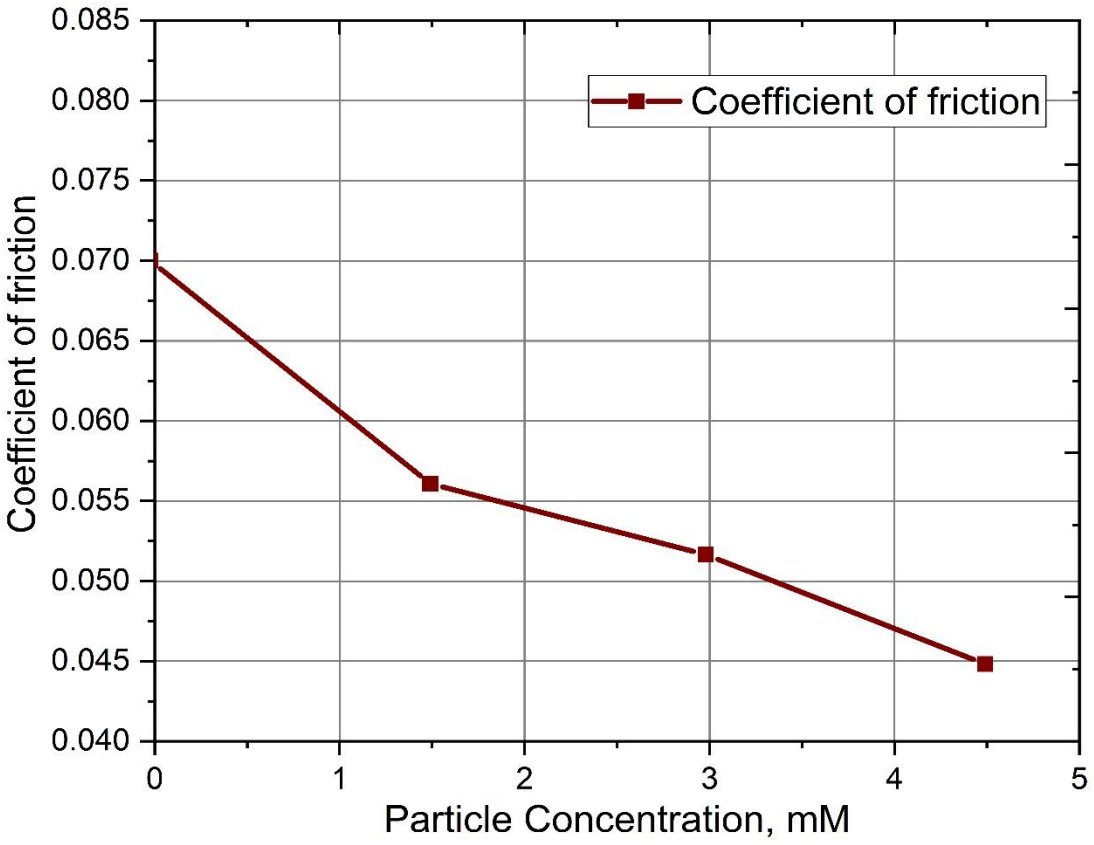

Figure 3.13: Coefficient of friction versus particle concentration in mM

Figure 3.14 shows the result of wear induced volume versus nanoparticle concentration. As shown in graph when particle concentration increased from 0 to 1, wear dropped from 0.050 to 0.043. And particle concentration increased from 1 to 3, wear dropped from 0.043 to 0.032. And when particle concentration increased further it enhances the wear. Both friction and wear reduced up to 35%.

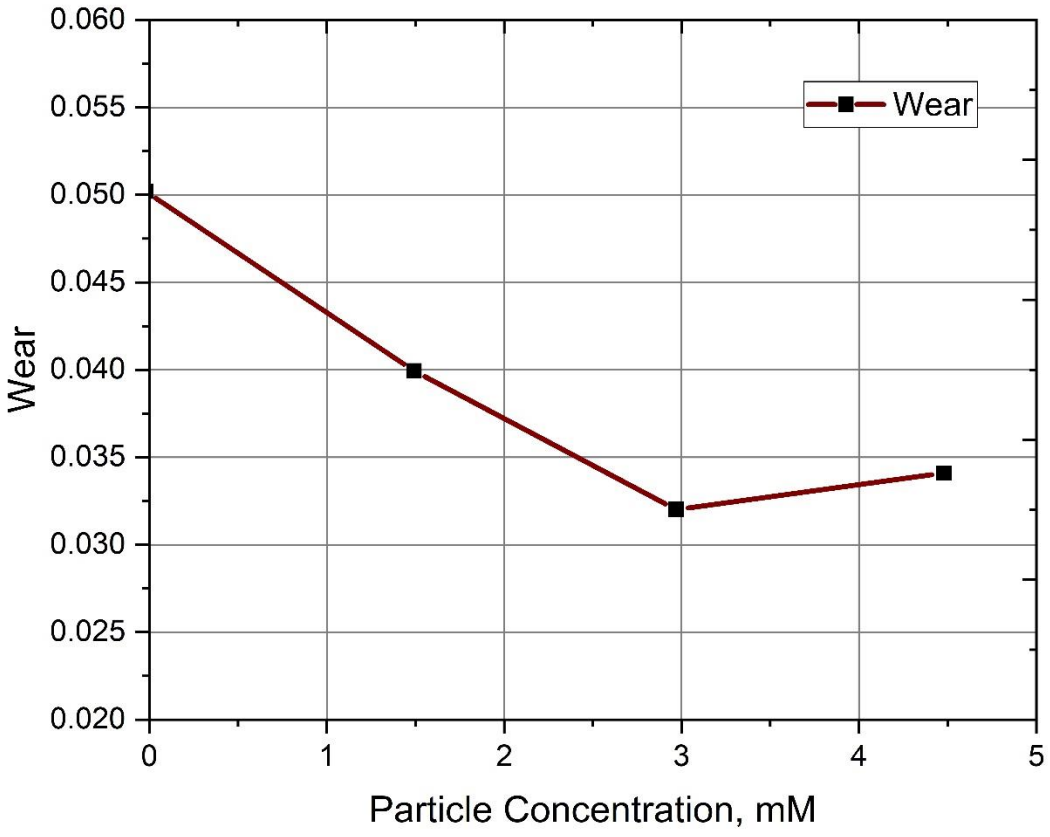

Figure 3.14: Wear versus particle concentration in mM

Figure 3.15 displayed the results of coefficient of friction versus time duration (cycles) at external load of 20N. In this case base lubricant shows marginally good results as compared to nanolubricant. But when this test is carried out under the time duration of 2000 to 2500, both curve will show approximately same results.

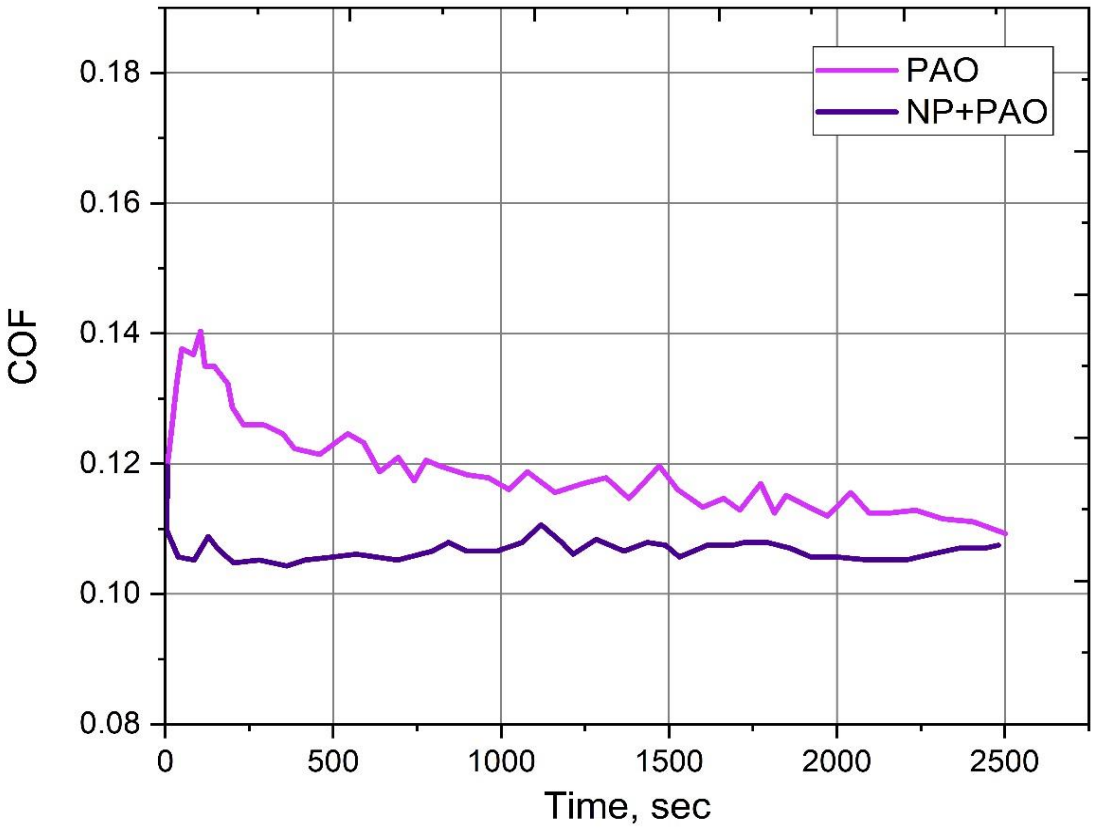

Figure 3.15: Coefficient of friction versus time duration of test at external load of 20N

Figure 3.16 displayed the results of coefficient of friction versus time duration when external load is 50N. When load is raised to 50N from 20N, now nanolubricant show better coefficient of friction results as compared to when apply external load of 20N. Here these two curves will not meet up at one point.

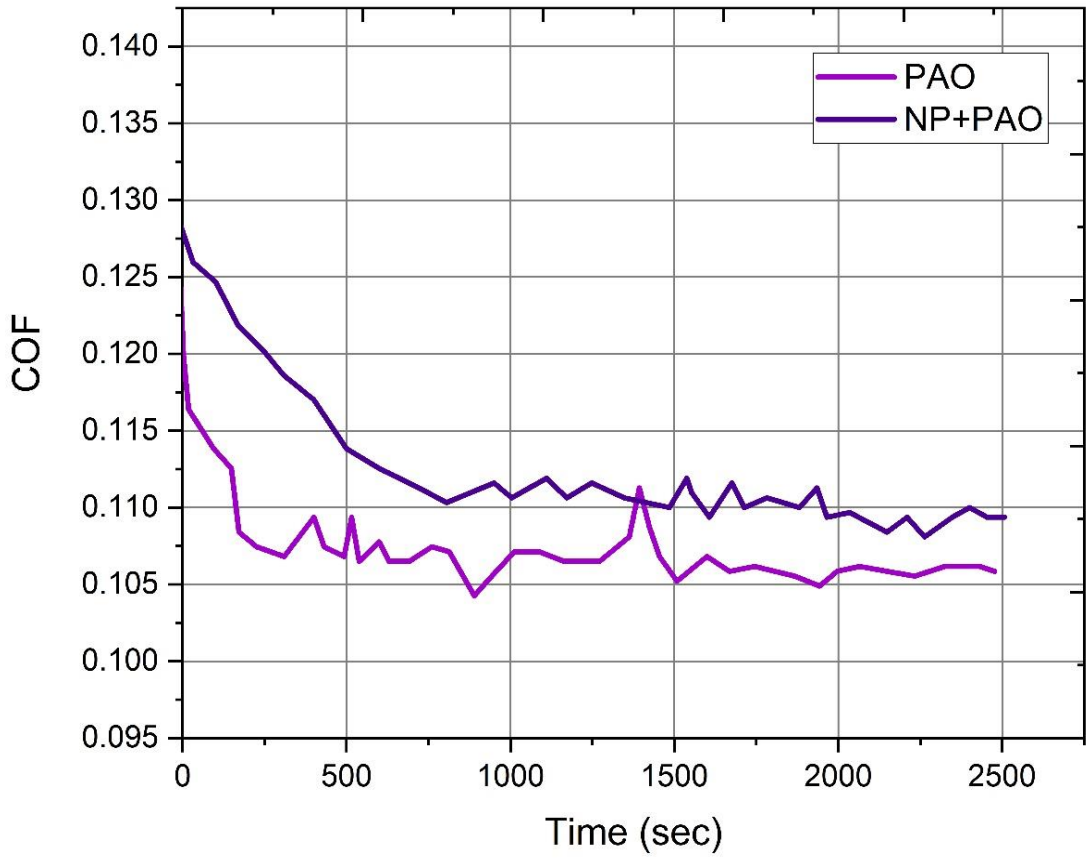

Figure 3.16: Coefficient of friction versus time duration when external applied load is 50N

Figure 3.17 displayed the results of COF versus different concentration of base lubricant & nanolubricant at normal load of 20N and 50N. Particles enhances friction at lower load of 20N while particle decrease friction at higher load. While base lubricant PAO show lower coefficient of friction at lower load while show high COF at higher load.

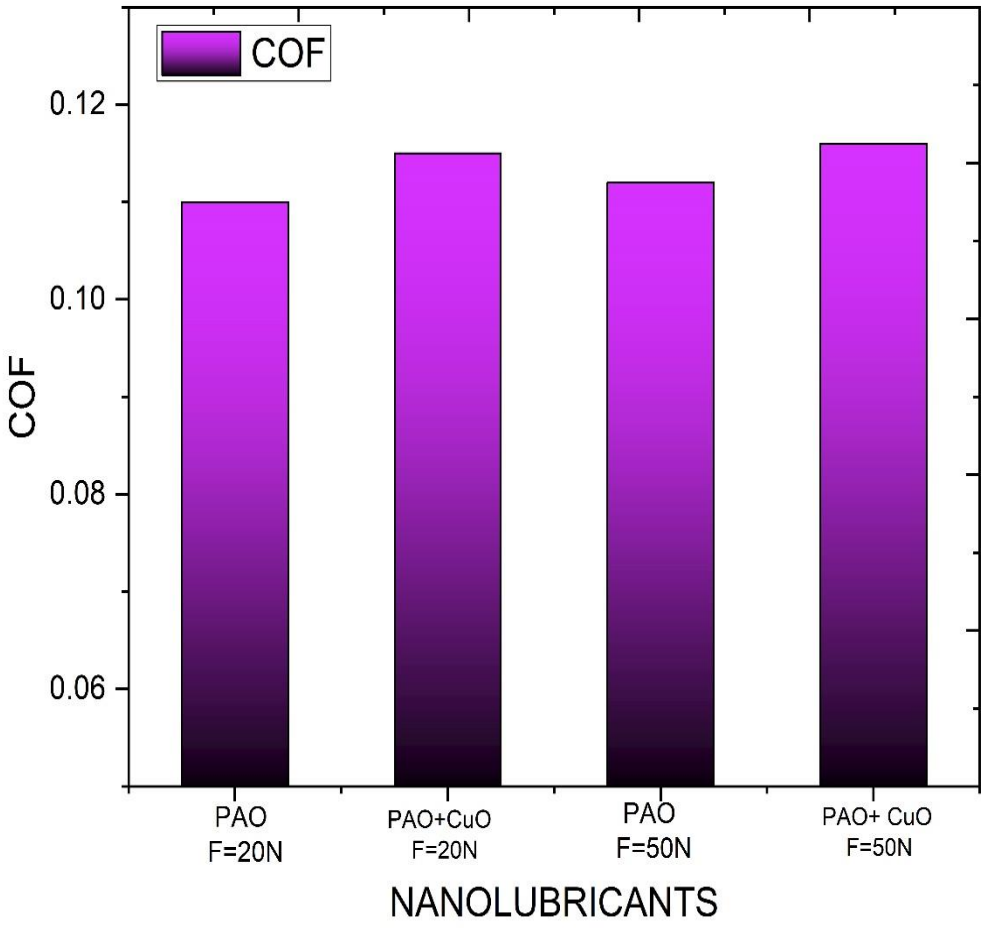

Figure 3.17: COF versus different concentration of base lubricant & nanolubricant at normal load of 20N and 50N.

Figure 3.18 displayed the results of wear versus different concentration of base lubricant and nanolubricant at normal load of 20N and 50N. Nanoparticles don't produce any effect on wear when external applied load is 20N. While nanoparticles decrease wear when external applied load is 50N. While base lubricant PAO shows less wear at lower load of 20N while shows higher wear at higher load of 50N.

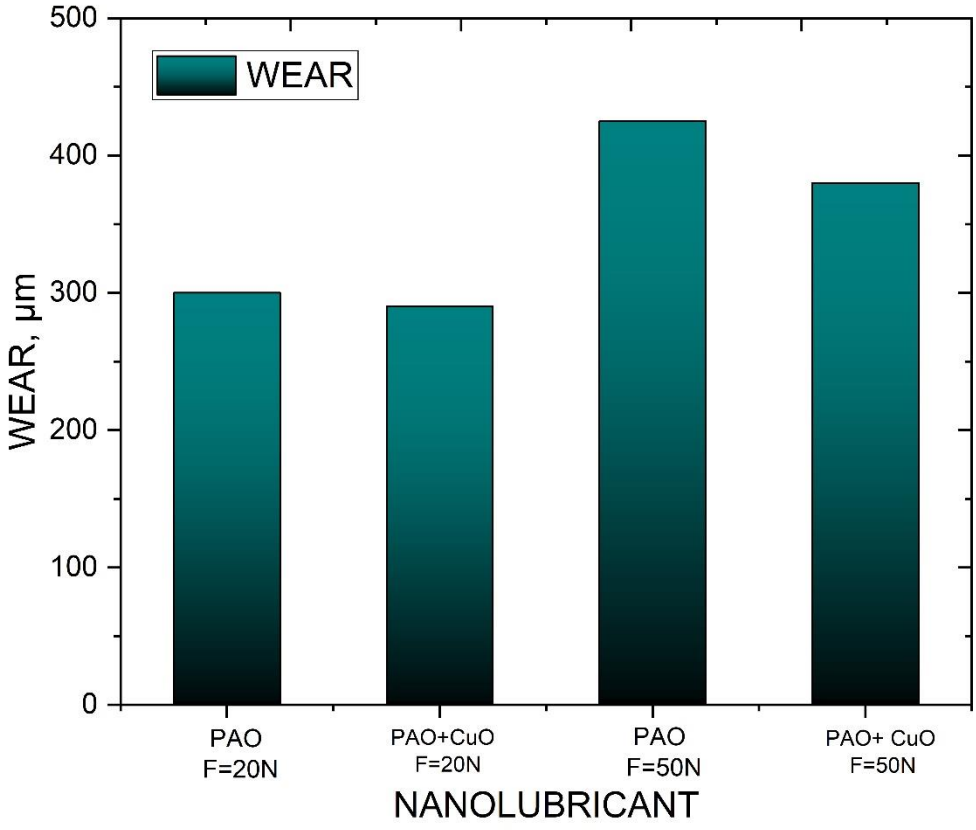

Figure 3.18: Wear versus different concentration of base lubricant and nanolubricant at normal load of 20N and 50N.

Figure 3.19 displayed the results of COF versus different concentration of base lubricant & nanolubricant at normal load of 20N, 50N & 150N. Base lubricant PAO shows approximately same wear when applied external load of 20N, 50N and 150N. While nanolubricant shows higher COF at lower load of 20N while nanolubricant shows lower COF at higher load of 50N. It again shows higher COF at higher load of 150N & same trends goes this way.

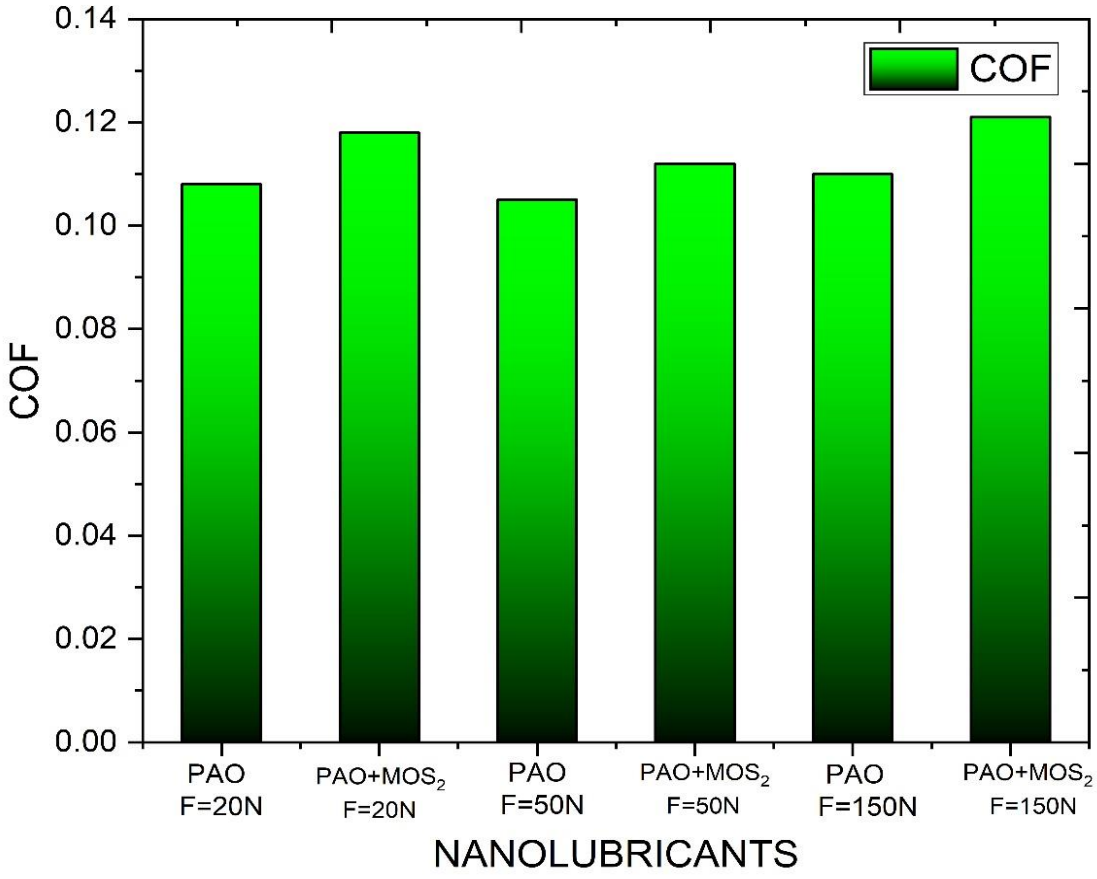

Figure 3.19: COF versus different concentration of base lubricant & nanolubricant at normal load of 20N, 50N and 150N.

Figure 3.20 displayed the results of wear versus different concentration of base lubricant and nanolubricant at normal load of 20N, 50N and 150N. Base lubricant PAO show less wear at lower load of 20N while wear enhances when applied load is greater than 50N and 150N. While as compared to base lubricant PAO, nanolubricant show less wear. Nanolubricant at lower load show less wear while wear increases when external applied load is greater than 20N.

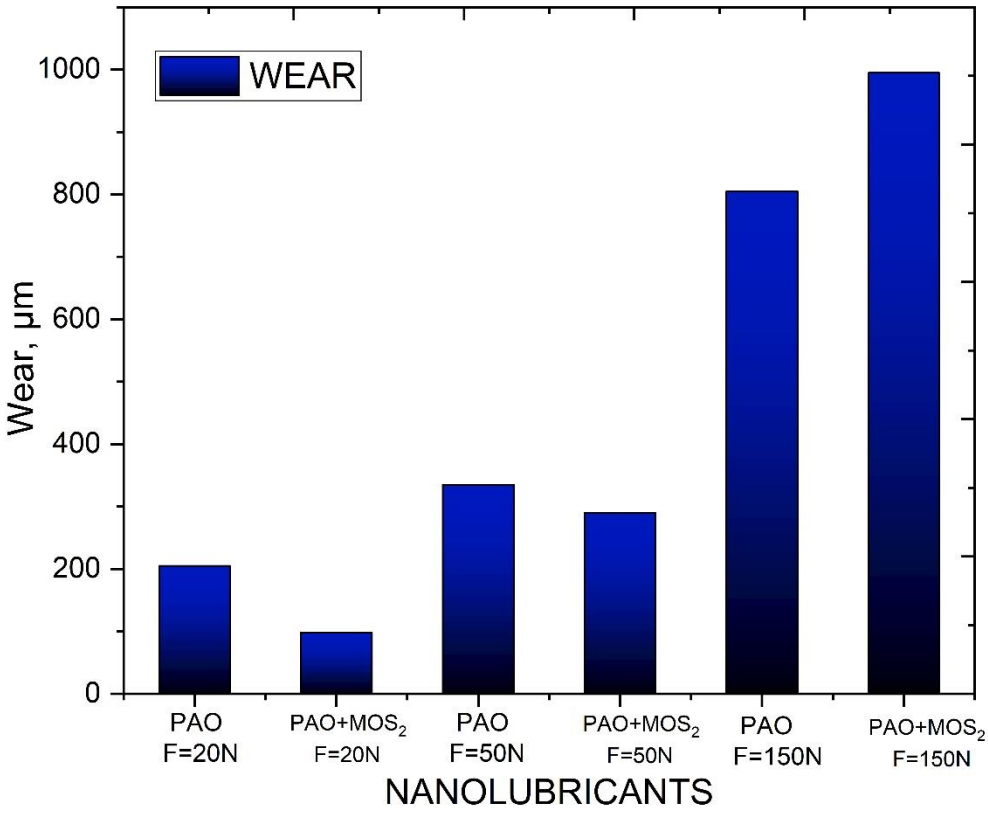

Figure 3.20: Wear versus different concentration of base lubricant and nanolubricant at normal load of 20N, 50N and 150N

CHAPTER 4: CONCLUSION

A multiscale model is developed for Molybdenum disulfide nanoparticles in Polyalphaolefin base oil. Rough surface contact sub-model based on micrometer sized roughness features and statistical contact sub-model of nanoparticles of size 40nm to 120 nm, in between rough surfaces are considered. Rough surface contact model is used to find average contact pressure and real area of contact. Statistical contact model is used to find void area around nanoparticles, force on nanoparticles and deformation of particles. Mathematical model of COF and wear are discussed.

Results show that the derived analytical results are in good agreement with previously available experimental results. The studied nano lubricant formulation reduces COF and wear in Boundary Lubrication regime. Incorporation of nanoparticles separate the rough surfaces which in turn reduces the real area of contact. As hard particles cause abrasive wear on bearing surfaces. Incorporation of larger particles can reduce abrasive wear but in some cases, it enhances friction coefficient. Results show an increase in wear up to the 1.0 %wt concentration of nanoparticles and a decrease as particle concentration increased up to 2.0 %wt. Since wear is larger at the 1.0 %wt fraction of nanoparticles and minimum at 2.0 %wt fraction, the result suggests that addition of naolubricant increase wear in some cases while in other cases it reduced wear. When particles are highly engaged in the rough surfaces, they keep the surfaces apart which in turn reduces the real area of contact. As more nano lubricant are introduced in the surfaces, more nanoparticles are engaged in contact which explain the monotonic reduction in COF. Also due to high contact pressure these nanoparticles can cause abrasive wear. As nanoparticle concentration enhances in between rough surfaces, more nanoparticles are in contact which in turn results in decreasing average particle/surface contact pressure. Nano lubricant should be stable to avoid these kinds of effects like precipitation, aggregation and clustering effect. Concentration of nano lubricant is restricted to 2.0 %wt so try to avoid this type of effect. The technique of decreasing real area of contact needs further investigation.

Reality is that there are many models which can reduced friction and wear. This model can be further be improvised. Third body contact model is exceptional as it connect nanolubricant properties. Molybdenum disulphide nanoparticles can provide guidelines for future experimental work and lubrication. Well accurately experiments concentrated on the mechanism proposed by this model and verify the exact mechanism. The results elaborated in this paper are only valid for the assumption expressed in this thesis and similar methodologies can be adopted to explore other nanoparticles.

Appendix I.

Table 2 contains the numerical values of the parameters used in the studies.

Table 2: Numerical values of the parameters used in the studies

Lubricants density	$\boldsymbol{\rho_{lub} = 0.761\ g/cc}$
Nanolubricant density	$\rho_{sol} = 0.7834\ g/cc$
Poisson ratio (Surface)	$v_S = 0.3$
nanoparticle Poisson ratio	$v_{NP} = 0.22$
Surface elastic modulus	$E_S = 198$ GPa
Particle elastic modulus	$E_{NP} = 162$ GPa
Yield strength (Surface)	Sy = 1.05 GPa
Effective Elastic modulus	E′ = 192 GPa

REFERENCES

[1] Sundus, F.; Fazal, M.A.; Masjuki, H.H. Tribology with biodiesel: A study on enhancing biodiesel stability and its fuel properties. Renew. Sustain. Energy Rev. **2017**, 70, 399–412.

[2] Amiri, M.; Khonsari, M.M. on the Thermodynamics of Friction and Wear—A Review. Entropy **2010**, 12, 1021–1049.

[3] Bruce, R.W. Handbook of Lubrication and Tribology, Volume II; CRC Press: Boca Raton, FL, USA, 2012; p. 1169.

[4] Jordan, H.; Kailyn, S.; Jason, D. Energy Education—Energy Loss. Available online: https://energyeducation.ca/encyclopedia/Energy_loss (accessed on 20 February 2020).

[5] U.S. Government. Where the Energy Goes: Gasoline Vehicles. Available online: https://www.fueleconomy.gov/feg/atv.shtml (accessed on 20 February 2020).

[6] Shafi, W.K.; Raina, A.; Haq, M.I.U. Friction and wear characteristics of vegetable oils using nanoparticles for sustainable lubrication. Tribal. Mater. Surf. Interfaces **2018**, 12, 27–43.

[7] Kalin, M.; Velkavrh, I.; Vižintin, J. The Stribeck curve and lubrication design for non-fully wetted surfaces. Wear **2009**, 267, 1232–1240. [CrossRef]

[8] Hamrock, B.J.; Schmid, S.R.; Jacobson, B.O. Fundamentals of Fluid Film Lubrication; CRC Press: Boca Raton, FL, USA, 2004.

[9] Maru, M.M.; Tanaka, D.K. Consideration of Stribeck Diagram Parameters in the Investigation on Wear and Friction Behavior in Lubricated Sliding. J. Braz. Soc. Mech. Sci. Eng. **2007**, 29, 55–62. [CrossRef]

[10] Rasheed, A.K.; Khalid, M.; Rashmi, W.; Gupta, T.C.S.M.; Chan, A. Graphene based nanofluids and nanolubricants—Review of recent developments. Renew. Sustain. Energy Rev. **2016**, 63, 346–362. [CrossRef]

[11] American Petroleum Institute (Ed.) Appendix E—API Base Oil Interchangeability Guidelines for Passenger Car Motor oils and Diesel Engine Oils; American Petroleum Institute: Washington, DC, USA, 2019; pp. 1–34.

[12] Speight, J.G. Chapter 3: Hydrocarbons from Crude Oil. In Handbook of Industrial Hydrocarbon Processes; Elsevier: Amsterdam, the Netherlands, 2020; pp. 95–142.

[13] Stachowiak, G.W.; Batchelor, A.W. Chapter 3: Lubricants and Their Composition. In Engineering Tribology, 3rd ed.; Elsevier: Amsterdam, the Netherlands, 2006.

[14] Wu, M.M.; Ho, S.C.; Forbus, T.R. Practical Advances in Petroleum Processing: Synthetic Lubricant Base Stock Processes and Products; Springer: New York, NY, USA, 2006.

[15] Nowak, P.; Kucharska, K.; Kaminski, M. Ecological and Health Ejects of Lubricant Oils Emitted into the Environment. Int. J. Environ. Res. Public Health **2019**, 16, 3002. [CrossRef] [PubMed]

[16] Salimon, J.; Salih, N.; Yousif, E. Biolubricants: Raw materials, chemical modifications and environmental benefits. Eur. J. Lipid Sci. Technol. **2010**, 112, 519–530. [CrossRef]

[17] Reeves, C.J.; Siddaiah, A.; Menezes, P.L. A Review on the Science and Technology of Natural and Synthetic Biolubricants. J. Bio-Tribo-Corros. **2017**, 3, 1–27. [CrossRef]

[18] Dai, W.; Kheireddin, B.; Gao, H.; Liang, H. Roles of nanoparticles in oil lubrication. Tribol. Int. **2016**, 102, 88–98. [CrossRef]

[19] Yang, G.; Zhang, Z.; Zhang, S.; Yu, L.; Zhang, P.; Hou, Y. Preparation and characterization of copper nanoparticles surface-capped by alkanethiols. Surf. Interface Anal. **2013**, 45, 1695–1701. [CrossRef]

[20] Padgurskas, J.; Rukuiza, R.; Prosy˘cevas, I.; Kreivaitis, R. Tribological properties of lubricant additives of Fe, Cu and Co nanoparticles. Tribol. Int. **2013**, 60, 224–232. [CrossRef]

[21] Asadauskas, S.J.; Kreivaitis, R.; Bikul˘cius, G.; Griguceviˇcien ˙ e, A.; Padgurskas, J. Tribological e_ects of Cu, Fe and Zn nano-particles, suspended in mineral and bio-based oils. Lubr. Sci. **2016**, 28, 157–176. [CrossRef]

[22] Flores-Castañeda, M.; Camps, E.; Camacho-López, M.; Muhl, S.; García, E.; Figueroa, M. Bismuth nanoparticles synthesized by laser ablation in lubricant oils for tribological tests. J. Alloys Compd. **2015**, 643,S67–S70. [CrossRef]

[23] Chou, R.; Battez, A.H.; Cabello, J.J.; Viesca, J.L.; Osorio, A.; Sagastume, A. Tribological behavior of polyalphaolefin with the addition of nickel nanoparticles. Tribol. Int. **2010**, 43, 2327–2332. [CrossRef]

[24] Peng, D.X.; Yuan, K.; Chen, S.-K.; Shu, F.-C.; Chang, Y.P. Dispersion and tribological properties of liquid para_n with added aluminum nanoparticles. Ind. Lubr. Tribol. **2010**, 62, 341–348. [CrossRef]

[25] Scherge, M.; Böttcher, R.; Kürten, D.; Linsler, D. Multi-Phase Friction and Wear Reduction by Copper Nanoparticle's. Lubricants **2016**, 4, 1–13. [CrossRef]

[26] Zhang, B.-S.; Xu, B.-S.; Xu, Y.; Gao, F.; Shi, P.-J.; Wu, Y.-X. CU nanoparticles effect on the tribological properties of hydrosilicate powders as lubricant additive for steel–steel contacts. Tribol. Int. **2011**, 44, 878–886. [CrossRef]

[27] Rajubhai, V.H.; Singh, Y.; Suthar, K.; Surana, A.R. Friction and wear behavior of Al-7% Si alloy pin under pongamia oil with copper nanoparticles as additives. Mater. Today Proc. **2019**, 25, 695–698. [CrossRef]

[28] Zhang, S.; Hu, L.; Feng, D.;Wang, H. Anti-wear and friction-reduction mechanism of Sn and Fe nanoparticles as additives of multialkylated cyclopentanes under vacuum condition. Vacuum **2013**, 87, 75–80. [CrossRef]

[29] Wang, J.; Guo, X.; He, Y.; Jiang, M.; Sun, R. The synthesis and tribological characteristics of triangular copper nanoplates as a grease additive. RSC Adv. **2017**, 7, 40249–40254. [CrossRef]

[30] Alves, S.M.; Barros, B.S.; Trajano, M.F.; Ribeiro, K.S.B.; Moura, E. Tribological behavior of vegetable oil-based lubricants with nanoparticles of oxides in boundary lubrication conditions. Tribol. Int. **2013**, 65, 28–36.[CrossRef]

[31] Wu, H.; Zhao, J.; Cheng, X.; Xia, W.; He, A.; Yun, J.-H.; Huang, S.; Wang, L.; Huang, H.; Jiao, S.; et al. Friction and wear characteristics of TiO2 nano-additive water-based lubricant on ferritic stainless steel. Tribol. Int.**2018**, 117, 24–38. [CrossRef]

[32] Wu, H.; Zhao, J.; Xia,W.; Cheng, X.; He, A.; Yun, J.-H.;Wang, L.; Huang, H.; Jiao, S.; Huang, L.; et al. A study of the tribological behaviour of TiO2 nano-additive water-based lubricants. Tribol. Int. **2017**, 109, 398–408.[CrossRef]

[33] Laad, M.; Ponnamma, D.; Sadasivuni, K.K. Tribological Studies of Nanomodified Mineral based Multi-grade Engine Oil. Int. J. Appl. Eng. Res. **2017**, 12, 2855–2861.

[34] Luo, T.; Wei, X.; Huang, X.; Huang, L.; Yang, F. Tribological properties of Al2O3 nanoparticles as lubricating oil additives. Ceram. Int. **2014**, 40, 7143–7149. [CrossRef]

[35] Peña-Parás, L.; Taha-Tijerina, J.; Garza, L.; Maldonado-Cortés, D.; Michalczewski, R.; Lapray, C. E_ect of CuO and Al2O3 nanoparticle additives on the tribological behavior of fully formulated oils. Wear **2015**, 332–333, 1256–1261. [CrossRef]

[36] Asrul, M.; Zulkifli, N.; Masjuki, H.; Kalam, M. Tribological Properties and Lubricant Mechanism of Nanoparticle in Engine Oil. Procedia Eng. **2013**, 68, 320–325. [CrossRef]

[37] Jatti, V.S.; Singh, T.P. Copper oxide nano-particles as friction-reduction and anti-wear additives in lubricating oil. J. Mech. Sci. Technol. **2015**, 29, 793–798.

[38] Song, X.; Zheng, S.; Zhang, J.; Li, W.; Chen, Q.; Cao, B. Synthesis of monodispersed ZnAl2O4 nanoparticles and their tribology properties as lubricant additives. Mater. Res. Bull. **2012**, 47, 4305–4310. [CrossRef]

[39] Azman, N.F.; Samion, S.; Sot, M.N.H.M. Investigation of tribological properties of CuO/palm oil nanolubricant using pin-on-disc tribotester. Green Mater. **2018**, 6, 30–37. [CrossRef]

[40] Xia, W.; Zhao, J.; Wu, H.; Jiao, S.; Zhao, X.; Zhang, X.; Xu, J.; Jiang, Z. Analysis of oil-in-water based nanolubricants with varying mass fractions of oil and TiO2 nanoparticles. Wear **2018**, 396–397, 162–171. [CrossRef]

[41] Rabaso, P.; Ville, F.; Dassenoy, F.; Diaby, M.; Afanasiev, P.; Cavoret, J.; Vacher, B.; Le Mogne, T. Boundary lubrication: Influence of the size and structure of inorganic fullerene-like MoS2 nanoparticles on friction and wear reduction. Wear **2014**, 320, 161–178. [CrossRef]

[42] Xu, Y.; Hu, E.-Z.; Hu, K.-H.; Xu, Y.; Hu, X. Formation of an adsorption film of MoS2 nanoparticles and dioctyl sebacate on a steel surface for alleviating friction and wear. Tribol. Int. **2015**, 92, 172–183. [CrossRef]

[43] Rosentsveig, R.; Gorodnev, A.; Feuerstein, N.; Friedman, H.; Zak, A.; Fleischer, N.; Tannous, J.; Dassenoy, F.; Tenne, R. Fullerene-like MoS2 Nanoparticles and Their Tribological Behavior. Tribol. Lett. **2009**, 36, 175–182.[CrossRef]

[44] Gulzar, M.; Masjuki, H.; Varman, M.; Kalam, M.; Mufti, R.; Zulkifli, N.; Yunus, R.; Zahid, R. Improving the AW/EP ability of chemically modified palm oil by adding CuO and MoS2 nanoparticles. Tribol. Int. **2015**, 88, 271–279. [CrossRef]

[45] Zhou, L.H.; Wei, X.C.; Ma, Z.J.; Mei, B. Anti-friction performance of FeS nanoparticle synthesized by biological method. Appl. Surf. Sci. **2017**, 407, 21–28. [CrossRef]

[46] Wan, Q.; Jin, Y.; Sun, P.; Ding, Y. Rheological and tribological behaviour of lubricating oils containing platelet MoS2 nanoparticles. J. Nanoparticle Res. **2014**, 16, 2386. [CrossRef]

[47] Zhang, L.L.; Tu, J.; Wu, H.; Yang, Y. WS2 nanorods prepared by self-transformation process and their tribological properties as additive in base oil. Mater. Sci. Eng. A **2007**, 454, 487–491. [CrossRef]

[48] Koshy, C.P.; Rajendrakumar, P.K.; Thottackkad, M.V. Evaluation of the tribological and thermo-physical properties of coconut oil added with MoS2 nanoparticles at elevated temperatures. Wear **2015**, 330–331,288–308. [CrossRef]

[49] Rabaso, P.; Ville, F.; Dassenoy, F.; Diaby, M.; Afanasiev, P.; Cavoret, J.; Vacher, B.; Le Mogne, T. Boundary lubrication: Influence of the size and structure of inorganic fullerene-like MoS2 nanoparticles on friction and wear reduction. Wear **2014**, 320, 161–178. [CrossRef]

[50] Kalin, M.; Kogovšek, J.; Remškar, M. Mechanisms and improvements in the friction and wear behavior using MoS2 nanotubes as potential oil additives. Wear **2012**, 280–281, 36–45. [CrossRef]

[51] Peng, D.; Kang, Y.; Hwang, R.; Shyr, S.; Chang, Y. Tribological properties of diamond and SiO2 nanoparticles added in para_n. Tribol. Int. **2009**, 42, 911–917. [CrossRef]

[52] Raina, A.; Anand, A. Lubrication performance of synthetic oil mixed with diamond nanoparticles: Elects of concentration. Mater. Today Proc. **2018**, 5, 20588–20594. [CrossRef]

[53] Gupta, M.K.; Bijwe, J. A complex interdependence of dispersant in nano-suspensions with varying amountof graphite particles on its stability and tribological performance. Tribol. Int. **2020**, 142, 105968. [CrossRef]

[54] Sivakumar, B.; Ranjan, N.; Sundara, R.; Kamaraj, M. Tribological properties of graphite oxide derivative as nano-additive: Synthesized from the waster carbon source. Tribol. Int. **2020**, 142, 105990. [CrossRef]

[55] Phiri, J.; Gane, P.; Maloney, T.C. General over view of graphene: Production, properties and application in polymer composites. Mater. Sci. Eng. B **2017**, 215, 9–28. [CrossRef]

[56] Eswaraiah, V.; Sankaranarayanan, V.; Ramaprabhu, S. Graphene-Based Engine Oil Nanofluids for Tribological Applications. ACS Appl. Mater. Interfaces **2011**, 3, 4221–4227. [CrossRef] [PubMed]

[57] Lin, J.;Wang, L.; Chen, G. Modification of Graphene Platelets and their Tribological Properties as a Lubricant Additive. Tribol. Lett. **2010**, 41, 209–215. [CrossRef]

[58] Zhao, J.; Mao, J.; Li, Y.; He, Y.; Luo, J. Friction-induced nano-structural evolution of graphene as a lubrication additive. Appl. Surf. Sci. **2018**, 434, 21–27. [CrossRef]

[59] Wang, X.; Zhang, Y.; Yin, Z.; Su, Y.; Zhang, Y.; Cao, J. Experimental research on tribological properties of liquid phase exfoliated graphene as an additive in SAE 10W-30 lubricating oil. Tribol. Int. **2019**, 135, 29–37.[CrossRef]

[60] Zhang, Z.-C.; Cai, Z.-B.; Peng, J.-F.; Zhu, M.-H. Comparison of the tribology performance of nano-diesel soot and graphite particles as lubricant additives. J. Phys. D: Appl. Phys. **2015**, 49, 045304. [CrossRef]

[61] Wu, B.; Song, H.; Li, C.; Song, R.; Zhang, T.; Hu, X. Enhanced tribological properties of diesel engine oil with Nano-Lanthanum hydroxide/reduced graphene oxide composites. Tribol. Int. **2020**, 141, 105951. [CrossRef]

[62] Wang, L.; Gong, P.; Li,W.; Luo, T.; Cao, B. Mono-dispersed Ag/Graphene nanocomposite as lubricant additive to reduce friction and wear. Tribol. Int. **2020**, 146, 106228. [CrossRef]

[63] Gan, C.; Liang, T.; Li,W.; Fan, X.; Zhu, M.-H. Amine-terminated ionic liquid modified graphene oxide/copper nanocomposite toward e_cient lubrication. Appl. Surf. Sci. **2019**, 491, 105–115. [CrossRef]

[64] Zhang, X.; Zhu, S.; Shi, T.; Ding, H.; Bai, Y.; Di, P.; Luo, Y. Preparation, mechanical and tribological properties of WC-Al2O3 composite doped with graphene platelets. Ceram. Int. **2020**, 46, 10457–10468. [CrossRef]

[65] Gulzar, M.; Masjuki, H.H.; Kalam, M.A.; Varman, M.; Zulkifli NW, M.; Mufti, R.A.; Zahid, R.; Yunus, R. Dispersion Stability and Tribological Characteristics of TiO2/SiO2 Nanocomposite-Enriched Biobased Lubricant. Tribol. Trans. **2016**, 60, 670–680. [CrossRef]

[66] An, V.V.; Anisimov, E.; Druzyanova, V.; Burtsev, N.; Shulepov, I.A.; Khaskelberg, M. Study of tribological behavior of Cu-MoS2 and Ag-MoS2 nanocomposite lubricants. SpringerPlus **2016**, 5, 72. [CrossRef] [PubMed]

[67] Wang, Z.; Ren, R.; Song, H.; Jia, X. Improved tribological properties of the synthesized copper/carbon nanotube nanocomposites for rapeseed oil-based additives. Appl. Surf. Sci. **2018**, 428, 630–639. [CrossRef]

[68] Ataie, S.A.; Zakeri, A. Improving tribological properties of (Zn–Ni)/nano Al2O3 composite coatings produced by ultrasonic assisted pulse plating. J. Alloys Compd. **2016**, 674, 315–322. [CrossRef]

[69] Li, S.; Qin, H.; Zuo, R.; Bai, Z. Friction properties of La-doped Mg/Al layered double hydroxide and intercalated product as lubricant additives. Tribol. Int. **2015**, 91, 60–66. [CrossRef]

[70] Meng, Y.; Su, F.; Chen, Y. Effective lubricant additive of nano-Ag/MWCNTs nanocomposite produced by supercritical CO2 synthesis. Tribol. Int. **2018**, 118, 180–188. [CrossRef]

[71] Li, S.; Qin, H.; Zuo, R.; Bai, Z. Friction properties of La-doped Mg/Al layered double hydroxide and intercalated product as lubricant additives. Tribol. Int. **2015**, 91, 60–66. [CrossRef]

[72] He, Q.; Li, A.; Guo, Y.; Liu, S.; Zhang, Y.; Kong, L. Tribological properties of nanometer cerium oxide as additives in lithium grease. J. Rare Earths **2018**, 36, 209–214. [CrossRef]

[73] Shen, T.; Wang, D.; Yun, J.; Liu, Q.; Liu, X.; Peng, Z. Tribological properties and tribochemical analysis of nano-cerium oxide and sulfurized isobutene in titanium complex grease. Tribol. Int. **2016**, 93, 332–346.[CrossRef]

[74] Hou, X.; He, J.; Yu, L.; Li, Z.; Zhang, Z.; Zhang, P. Preparation and tribological properties of fluorosilane surface-modified lanthanum trifluoride nanoparticles as additive of fluoro silicone oil. Appl. Surf. Sci. **2014**, 316, 515–523. [CrossRef]

[75] Liu, F.; Shao, X.; Yin, Y.; Zhao, L.; Shao, Z.; Liu, X.; Meng, X. Shape controlled synthesis and tribological properties of CeVO4 nanoparticles as lubricating additive. J. Rare Earths **2011**, 29, 688–691. [CrossRef]

[76] Lee, K.; Hwang, Y.; Cheong, S.; Choi, Y.; Kwon, L.; Lee, J.; Kim, S.H. Understanding the Role of Nanoparticles in Nano-oil Lubrication. Tribol. Lett. **2009**, 35, 127–131. [CrossRef]

[77] Viesca, J.L.; Battez, A.H.; González, R.; Chou, R.; Cabello, J.J. Antiwear properties of carbon-coated copper nanoparticles used as an additive to a polyalphaolefin. Tribol. Int. **2011**, 44, 829–833. [CrossRef]

[78] Wang, X.; Yin, Y.; Zhang, G.;Wang,W.; Zhao, K. Study on Antiwear and Repairing Performances about Mass of Nano-copper Lubricating Additives to 45 Steel. Phys. Procedia **2013**, 50, 466–472. [CrossRef]

[79] Zulkifli, N.; Kalam, M.; Masjuki, H.; Yunus, R. Experimental Analysis of Tribological Properties of Biolubricant with Nanoparticle Additive. Procedia Eng. **2013**, 68, 152–157. [CrossRef].

[80] Balaji, S.; AB, M.A.N. Tribological performance of graphene/graphite filled phenolic composites—A comparative study. Compos. Commun. **2019**, 15, 34–39.

[81] Liu, X.; Xu, N.; Li, W.; Zhang, M.; Chen, L.; Lou, W.; Wang, X. Exploring the effect of nanoparticle size on the tribological properties of SiO2/polyalkylene glycol nanofluid under different lubrication conditions.Tribol. Int. **2017**, 109, 467–472. [CrossRef]

[82] Greenwood, J. A., and Williamson, J. B. P., 1966, "Contact of Nominally Flat Surface," *Proc. Roy. Soc.* (London), Series A295, pp. 300–319.

[83] Greenwood, J. A., and Tripp, J. H., 1967, "The Elastic Contact of Rough Spheres," ASME *Journal of Applied Mechanics,* Vol. 34, pp. 153–159.

[84] Greenwood, J. A., and Tripp, J. H., 1970–1971, "The Contact of Two Nominally Flat Rough Surfaces," *Proc. Instn. Mech. Engrs.,* Vol. 185, pp. 625–633

[85] Greenwood, J. A., and Tripp, J. H., 1970–1971, "The Contact of Two Nominally Flat Rough Surfaces," *Proc. Instn. Mech. Engrs.*, Vol. 185, pp. 625–633

[86] Bush, A. W., Gibson, R. D., and Thomas, T. R., 1975, "The Elastic Contact of a Rough Surface," *Wear,* Vol. 35, pp. 87–111

[87] Bush, A. W., Gibson, R. D., and Keogh, G. P., 1979, "Strong Anisotropic Rough Surface," ASME JOURNAL OF TRIBOLOGY, Vol. 101, pp. 15–20

[88] Pullen, J., and Williamson, J. B. P., 1972, "On the Plastic Contact of Rough Surfaces," *Proc. Roy. Soc.* (London), A327, pp. 159–173

[89] Hernández Battez, A., et al., *Friction reduction properties of a CuO nanolubricant used as lubricant for a NiCrBSi coating.* Wear, 2010. **268**(1-2): p. 325-328.

[90] Alves, S.M.; Barros, B.S.; Trajano, M.F.; Ribeiro, K.S.B.; Moura, E. Tribological behavior of vegetable oil-based lubricants with nanoparticles of oxides in boundary lubrication conditions. Tribol. Int. **2013**, 65, 28–36.

[91] Yadgarov, L.; Petrone, V.; Rosentsveig, R.; Feldman, Y.; Tenne, R.; Senatore, A. Tribological studies of rhenium doped fullerene-like MoS2 nanoparticles in boundary, mixed and elasto-hydrodynamic lubrication conditions. Wear **2013**, 297, 1103–1110. [CrossRef]

[92] Ingole, S.; Charanpahari, A.; Kakade, A.; Umare, S.S.; Bhatt, D.V.; Menghani, J. Tribological behavior of nanoTiO2 as an additive in base oil. Wear **2013**, 301, 776–785. [CrossRef]

[93] Chong, W. and Curz, M. (2014) 'Elastoplastic contact of rough surfaces: a line contact model for boundary regime of lubrication' Research gate, pp-1178.

[94] Shafi, W.K.; Raina, A.; Haq, M.I.U. Friction and wear characteristics of vegetable oils using nanoparticles for sustainable lubrication. Tribol. Mater. Surf. Interfaces **2018**, 12, 27–43.

CERTIFICATE OF COMPLETENESS

It is hereby certified that the dissertation submitted by NS Hafiz Zia ur Rahman, Reg. No. **00000274875**, titled: ***Numerical Investigation of Friction and Wear Characteristics of Surfaces using MoS_2 Nanoparticles in* PAO** has been checked/reviewed, and its contents are complete in all respects.

Supervisor's Name: Dr. Raja Amer Azim Signature: _____

Date: _____